Title
T Cell Antigen Discovery Using Soluble Vaccinia Proteome Reveals Recognition of Antigens with Both Virion and Nonvirion Association

Journal
The Journal of Immunology, 193(4)

ISSN
0022-1767

Authors
Davies, D Huw
Chun, Sookhee
Hermanson, Gary
et al.

Publication Date
2014-08-15

DOI
10.4049/jimmunol.1400663

Peer reviewed

Published in final edited form as:
J Immunol. 2014 August 15; 193(4): 1812–1827. doi:10.4049/jimmunol.1400663.

T cell antigen discovery using soluble vaccinia proteome reveals recognition of antigens with both virion and non-virion association*

D. Huw Davies[a,b], **Sookhee Chun**[a], **Gary Hermanson**[b], **Jo Anne Tucker**[c], **Aarti Jain**[a], **Rie Nakajima**[a], **Jozelyn Pablo**[a,b], **Philip L. Felgner**[a], and **Xiaowu Liang**[b]

[a]Division of Infectious Diseases, School of Medicine, University of California Irvine, Irvine CA, 92697

[b]Antigen Discovery Inc., Irvine, CA 92618

[c]Division of Hematology & Oncology, School of Medicine, University of California Irvine, Irvine CA, 92697

Abstract

Vaccinia virus (VACV) is a useful model system for understanding the immune response to a complex pathogen. Proteome-wide antibody profiling studies reveal the humoral response to be strongly biased towards virion associated antigens, and several membrane proteins induce antibody-mediated protection against VACV challenge in mice. Some studies have indicated the CD4 response is also skewed toward proteins with virion association, whereas the CD8 response is more biased toward proteins with early expression. In this study, we have leveraged a VACV-WR plasmid expression library, produced previously for proteome microarrays for antibody profiling, to make a solubilized full VACV-WR proteome for T cell antigen profiling. Splenocytes from VACV-WR-infected mice were assayed without prior expansion against the soluble proteome in assays for Th1 and Th2 signature cytokines. The response to infection was polarized toward a Th1 response, with the distribution of reactive T cell antigens comprising both early and late VACV proteins. Interestingly, the proportions of different functional subsets were similar to that present in the whole proteome. In contrast, the targets of antibodies from the same mice were enriched for membrane and other virion components, as described previously. We conclude that a 'non-biasing' approach to T cell antigen discovery reveals a T cell antigen profile in VACV that is broader and less skewed to virion-association than the antibody profile. The T cell antigen mapping method developed here should be applicable to other organisms where expressible 'ORFeome' libraries are also available, and is readily scalable for larger pathogens.

Introduction

Understanding which proteins within the proteome of a pathogen engender antibodies and T cell responses, sometimes collectively referred to as the "immunome", is vital for the design

*This work was supported in part by NIH/NIAID grants R43AI063728, U54AI065359 and Antigen Discovery Inc.

Corresponding Author: D. Huw Davies, PhD, University of California Irvine, Department of Medicine, Division of Infectious Diseases, Irvine, CA 92697, lab 949 824-4932, fax 949 824 7387, cell 949 296-5620, ddavies@uci.edu.

of safer alternatives to live attenuated vaccines (1-3). Screening proteomes for T cell antigens is more complex than for antibodies, in part because of the relative complexity of T cell assays that require live T cell responders, and the challenges of obtaining the proteome in a format compatible with cell viability.

The use of synthetic peptides to substitute for the products of natural antigen processing displayed on the surface of APCs has been available since the mid-1980s (4). However, the cost of peptide synthesis effectively precludes proteome-wide searches of all but the smallest viruses. This has been a major impetus behind the development of predictive algorithms for locating putative T cell epitopes based on MHC allele-specific binding motifs, TAP transporter binding motifs, and known processing enzyme cleavage sites (5, 6). A manageable number of candidate epitopes can then be selected and tested experimentally with panels of overlapping synthetic peptides. Curated databases of experimentally-defined epitopes help refine these algorithms (7-9). The elution of MHC I and II-bound peptides from APCs followed by sequencing by mass spectrometry (10, 11) is also a means for identifying potential T cell epitopes and the antigens they are derived from at the proteomic level (12-14). In recent years expression libraries created from genomic fragments or PCR amplified ORFs (so-called “ORFeomes”) have also been brought to bear on the problem of proteome-wide T cell screening. For CD4 T cells, which require exogenous antigen for uptake and processing by APCs, libraries expressed in E coli have proven very useful. Steps must be taken to mitigate mitogenicity of contaminants, either by dilution (15, 16), cellular sequestration (17), or high throughput (HT) purification (18-21). For CD8 cells the challenge is the development of HT delivery of antigen or antigen transgenes into the cytosol of APCs and screening for protein expression. This has been achieved in HSV where transgenes are cloned with an in-frame GFP protein to allow rapid confirmation of intracellular expression (22-24).

In the 20th century, vaccinia virus (VACV) was used as a vaccine to prevent, and finally eradicate, smallpox, a disfiguring and often fatal disease caused by the related orthopoxvirus, variola (VARV). VACV has been widely used as a model infection to understand vaccine-engendered immunity and memory, and is helping to forge the technologies for many HT immunomic technologies (reviewed in (25, 26)). VACV has a double-stranded DNA genome that encodes ~220 proteins, of which more than a third are structural (virion-associated) components expressed late in the infection cycle. The remaining proteins are early or intermediate gene products that are expressed in infected cells and have functions in DNA replication, transcription and host cell interactions. Antibody targets are predominantly directed toward membrane proteins and other virion components (25). This finding is entirely consistent with the requirement for antibodies to target surface-accessible structures to neutralize virus and trigger complement-mediated effector functions. Less is known about the CD4 T cell response to VACV. Given the requirement by B cells for CD4 ‘helper’ T cells to produce antibodies, there is an expectation that the dominance of antibodies to late proteins with virion association would be reflected in the CD4+ compartment also.

To address a general need for proteome-wide approaches to T cell antigen mapping, we aimed to develop a HT protein expression and purification method that was compatible with

CD4 T cell assays. The starting point for this study was a plasmid library comprising ~220 different VACV-WR ORFs. The most recent iteration of the library has been expressed in small scale (10-50μl) *in vitro* transcription/translation (IVTT) reactions for antibody (27, 28) and T cell (15, 16) antigen profiling studies in DryVax® vaccinees. A few potentially diagnostic antigens were also produced in larger quantities expressed from the same plasmids as SDS-solubilized inclusion bodies (IBs) in *E. coli* BL21 cells, as a low-cost alternative to expression in IVTT (27). Because a generic purification method was used for the latter, we have adapted it here to a HT 96-well format which enabled the entire VACV-WR proteome to be purified simultaneously. T cells were then obtained for antigen profiling directly from VACV-WR infected mice without prior expansion *in vitro*. Moreover, no predictive approaches to antigen discovery were necessary. The results of this 'non-biasing' approach reveal a profile of T cell antigens this is wider and less skewed toward virion association than predicted by the antibody profile alone.

Materials and Methods

Antibodies and other reagents

Paired capture and biotinylated detection antibodies for mouse IFN-γ ELISPOTs were purchased from Pharmingen (clones R4-6A2 Cat# 551216, and XMG1.2 Cat # 554410, respectively). Biotinylated goat anti-mouse IgG, IgG1 and IgG2c secondary antibodies were purchased from Jackson ImmunoResearch (Cat# 115-065-008, 115-065-205, and 115-065-208, respectively). For monitoring protein expression on arrays, monoclonal mouse anti-polyhistidine ('HIS'; clone His-1, from Sigma Cat # H1029) and rat anti-hemagglutinin ('HA'; clone 3F10, anti-HA high affinity, Roche Cat# 11 867 423 001) were used. Strepatavidin-alkaline phosphatase for ELISPOTs was purchased from Pharmingen (Cat# 554065). Streptavidin-conjugated SureLight® P-3 was purchased from Columbia Biosciences (Cat# D7-2212). CpG and GpC oligonucleotides were purchased from Coley Pharmaceuticals Inc. Immunostimulatory complexes (ISCOMs, AbISCO-100) were purchased from Isconova, Sweden. Magpix beads for Luminex-based cytokine assay of murine IFNγ, IL2, IL4 and IL5 were purchased from Millipore.

Construction of vaccinia expressible proteome and protein microarrays

The high throughput ligase-free cloning platform has been described previously (29). Briefly, custom PCR primers comprising 20 base pairs of gene-specific sequence with 33 base pairs of "adapter" sequences were used in PCR reactions with vaccinia WR genomic DNA as template. The adapter sequences, which become incorporated into the termini flanking the amplified gene, are homologous to the cloning site of the linearized T7 expression vector pXi and allow PCR products to be cloned by *in vivo* homologous recombination in competent DH5α cells. The resulting protein incorporates a 5′ HIS epitope, an ATG translation start codon, and a 3′ HA epitope and T7 terminator. Arrays for this study (Antigen Discovery Inc., Irvine, CA) used a second iteration of the ORFeome library that was re-cloned and sequence-verified as part of a contract to profile sera from several NIH-sponsored clinical trials (27, 28). For arrays, the library was weeded of 27 of the 29 non-seroreactive pseudogenes, and the remaining ORFs were expressed in cell free *in vitro* transcription/translation (IVTT) reactions (RTS-100 from 5 Prime Inc.) according to the

manufacturer's instructions. In addition, 31 membrane proteins and other components of the fusion/entry complex were also expressed in RTS-100 disulfide kits (5-Prime). Purified WR148/− and WR101/H3L were also printed in serial dilutions. (Nomenclature used for each ORF is a concatenation of both the Copenhagen and Western Reserve gene IDs). Details of the array used in this study have been deposited in the Gene Expression Omnibus (GEO) archive under accession number GPL15100 (http://www.ncbi.nlm.nih.gov/geo/query/acc.cgi?acc=GPL15100).

Protein purification and quantification

Sequence verified second generation VACV-WR expression plasmids were transformed into BL21 cells, and master cell bank (MCB) stocks made from overnight cultures frozen in 25% glycerol in 96 well plates. For large protein preps (for immunizations) expression was autoinduced in *E. coli* strain BL21 cells and proteins purified either as SDS-solubilized inclusion bodies or on conventional nickel-chelate columns as described (27). Two forms of WR101/H3L were produced for immunizations: one full length protein and one lacking transmembrane and cytoplasmic amino acids ("H3L" and "H3LΔTM" respectively). Proteins were quantified using the Pierce® BCA Protein Assay Kit (Thermo Scientific) according to the manufacturer's instructions. This method was used as it is insensitive to the presence of any SDS in the proteins. Briefly, 10µl of protein sample was mixed with 200µl of Working Reagent, in a 96-well plate, thoroughly mixed by vortexing for 30 seconds and incubated at 37°C for 30 minutes by floating in a water bath. The absorbance of the reaction was measured at 562nm and the quantity of each protein determined from a calibration curve of known concentrations of BSA. Endotoxin content was quantified in a sample of purified IB preps using a commercial *Limulus* amebocyte lysate (LAL) assay (QCL-1000® from Lonza, Walkersville, MD) according to the manufacturers' instructions. A calibration curve was constructed from 4 dilutions of a standard positive control supplied with the kit of 1.0, 0.5, 0.25 and 0.1 EU/ml. The values of the IB samples tested were in the range 0.1-0.3 EU/ml or below (data not shown).

High throughput purification and solubilization of inclusion bodies (IBs)

A miniaturized version of the IB expression and purification procedure (27) was developed. Transformed BL21 cells from frozen MCB stocks were first inoculated using a multichannel pipette into flat-bottomed 96-well blocks (Qiagen) containing 1ml LB medium with 100µg/ml kanamycin and incubated overnight (18-24 hrs) at 37°C with shaking at 650rpm to generate live seed cultures. These were then used to inoculate 1-2µl into 96-well blocks containing 1ml MagicMedia (Invitrogen) with 100µg/ml kanamycin. These were incubated overnight as before to allow auto-expression of protein and inclusion body (IB) formation. The following day, the cultures were harvested by centrifugation for 10 mins at 6,000 × g, 4°C, and the cells disrupted by vortexing in 200µl BugBuster ('BB') supplemented with 1µl/ml benzonase (Novagen Cat# 70746), 1µl/30ml lysozyme (Novagen Cat# 71110) to a final conc. of 1,000 U/ml, and one protease inhibitor pill/50ml (Roche Cat #04693132001). The block was then incubated at RT for 20 mins with occasional vortexing until the solution was clear and not viscous. IBs were then pelleted at 5,000 × g for 15 mins at 4°C, resuspended in 200µl BB master mix, and incubated for a further 20 mins with periodic vortexing. An additional 200µl of 0.1x BB master mix was then added and the block

vortexed and the IBs pelleted by centrifugation as before. The pellet was washed in 400μl 0.1x BB master mix, incubated for 5 mins at RT, and the IBs pelleted by centrifugation. After discarding the supernatant, IBs were solubilized in 200μl of 0.2% SDS in PBS and placed at 4°C until clear (usually overnight). Proteins that were not solublized at this time were usually solubilized by raising the SDS concentration to 0.3-0.4%. Free SDS was then precipitated by addition of 8μL 1M KCl per 200μl protein solution (final conc. 40mM) and placed on ice for at least 10 min to precipitate the detergent. The SDS was then removed by centrifugation for 20 mins at 6,000 × g at 4°C, and 150μl of the supernatant (solubilized IB protein) decanted into a 96-well plate containing 30μl of 50% glycerol, and stored at −80°C until required for use for cellular assays. Expression of the IB preparations was verified by printing the IBs preparations onto microarrays, followed by indirect immunofluorescence of the N-terminal 10x polyhistidine (HIS) and C-terminal YPYDVPDYA influenza hemagglutinin (HA) epitope tags incorporated into each vaccinia ORF as described (29). Slides were scanned and a cutoff signal defined using the mean+2SD of 8 replicate spots of carrier buffer alone.

Mouse immunizations

Purified VACV proteins were formulated with CpG/ISCOMs or alum as adjuvants. For CpG/ISCOMs, 250μl pre-formed ISCOMs at 0.48mg/ml (Abisco-100 from ISCONOVA, Sweden) and 6.2μl CpG at 20.05mg/ml (ODN-1826 from Coley Pharmaceuticals Inc) were combined first and then mixed with 250μl solubilized recombinant protein antigen in PBS (0.4mg/ml). The formulation was mixed by shaking and 50μl injected into each gastrocnemius muscle of a C57Bl/6 mouse (=total 20μg of antigen per mouse). For alum, 25μl of solubilized antigen at 0.4mg/ml in PBS was combined with an equal volume of aluminum hydroxide gel (Sigma-Aldrich). The formulation was and mixed by end-over-end rotation at 4°C for 30 minutes and 50μl then injected into each gastrocnemius muscle of a C57Bl/6 mouse. As a source of antigen-specific T cells to develop the high throughput (HT) antigen screen, we immunized mice against VACV antigens. These were delivered either as individual recombinant proteins formulated in adjuvant, or viable or inactivated VACV strain WR (VACV-WR) as follows. Recombinant proteins were administered i.m. in PBS adjuvanted in CpG/ISCOMs or alum as described above, and boosted with identical formulations once or twice at 14 day intervals via the same route. For VACV-WR infections, mice were given ~5×10^5 pfu in 100μl by the i.p. route. Inactivated VACV-WR was prepared by incubating vials of virus containing 1ml at 10^9 pfu/ml to 65°C for 1h in a water bath, and non-viability confirmed by plaque assay. Mice were administered ~1×10^7 pfu equivalents of heat inactivated VACV-WR emulsified in ISCOM/CpG or alum by i.p. route. In each case, immunized mice were then challenged using 5×10^5 pfu of viable VACV-WR administered i.n. in a volume of 10μl to the nare. Mice were weighed daily and any that lost >25% of their original body weight were euthanized. On day 10-14 after the i.n. challenge, mice were sacrificed and tissues harvested for serological and T cell assays.

Cytokine assays

ELISPOTs were conducted mouse T cell medium (TCM) comprising Iscove's Modified Dulbecco's Medium (IMDM) supplemented with 5×10^{-5} M β-mercaptoethanol, 2mM L-glutamine, 100 IU penicillin/ml, 100μg streptomycin per ml (all from Invitrogen), and 10%

batch-tested FCS (GIBCO). ELISPOT plates (Millipore Milliscreen 96 well plates; cat # MAHAS45) were prepared by coating in 2μg/ml anti-mouse IFN-γ capture antibody in carbonate buffer pH9.6, overnight at 4°C. The following day, plates were washed 3x in sterile phosphate buffered saline/0.05% Tween 20 (T-PBS) followed by 3x in sterile PBS, and then blocked with IMDM containing 10% batch-tested FCS, 200μl/well, for 1-2h in a tissue culture incubator. After blocking, the contents of the plate were discarded and solublized IBs added to the plate at 1/10 dilution in TCM (100μl/well) or titrated in TCM by four 3-fold serial dilutions starting at 1/10 dilution. Control wells contained SDS-solubilized extracts of BL21 cells transformed with non-recombinant pXi vector or from untransformed cells. Single cell suspensions were then added (50μl/well), from either draining lymph nodes or from spleens depleted of erythrocytes using ACK lysing Buffer (Lonza Cat# 10-548E), giving a final concentration of 5×10^5 cells/well and a final dilution of solubilized IBs of 1/20, and maintained at 37°C/5% CO_2 in a humidified incubator. Duplicate wells of cells containing concanavalin A (Sigma) at a final concentration of 1μg/ml were used for viability controls. After 18h incubation the supernatants were harvested and frozen for future cytokine assay, and plates washed 4x in T-PBS. After incubation for 2h at RT in biotinylated IFN-γ detection antibody in T-TBS/1% BSA, 50μl/well, plates were washed 4x in T-PBS and incubated in streptavidin-alkaline phosphatase diluted 1/1000 in T-PBS/1% BSA for 30 mins. After washing 3x in T-TBS and 3x in TBS, spots were developed for 10-15 mins in 1-Step™ NBT/BCIP developer (Thermo Scientific), rinsed briefly in distilled water, and allowed to dry. Numbers of IFN-γ-producing cells/well were quantified using an iSPOT plate reader (Advanced Imaging Devices GmbH). IL2, IFNγ, IL4 and IL5 were also quantified in supernatants using the Luminex® MagPix® multiplexing system with reagents from EMD/Millipore and used according to the manufacturer's instructions.

Data analysis

For ELISPOT data, a cutoff was defined as the average +2.5SD of 24 control ('irrelevant') antigens from *Plasmodium falciparum* (30) and *Francisella tularensis* (31), both produced as solubilized SDS-IBs from expression plasmids. Fisher's exact test (graphpad.com) was used to test the significance of enrichment of functional subsets within IgG and T cell profiles (32). Cytokine concentrations in culture supernatants were determined from titrations of cytokine standards supplied with the MagPix kits using the Luminex® software. For array data, raw signal intensities were subtracted of the average of controls spots (IVTT reactions lacking template DNA). Normally a cutoff for seropositivity was defined as the average + 2SD of the entire antigen spots seen by a population of naïve individuals. However, sera from naïve mice give essentially blank arrays. Therefore an arbitrary cutoff of 5,000 was used, which is close to the average +2SD of the bottom 25% of antigens when ranked by the average of 8 infected mice. The significance of overlap in protein sets identified by different screening assays (such as IFNγ by ELISpot vs. Luminex®) was determined using the dhyper function in R.

Results

Evaluations of the immunogenicity of purified VACV-WR proteins

The starting point for this study was an expression plasmid library comprising 225 different VACV-WR ORFs. The IVTT library has been expressed in cell-free *E. coli*-based *in vitro* transcription/translation (IVTT) reactions previously, for both antibody and T cell profiling in vaccinees receiving the licensed smallpox vaccine, DryVax® (15, 16, 27, 28). Previously we also expressed and purified a small number of the antibody targets in mg quantities in transformed *E. coli* BL21 cells for ELISA assay development (27). Each protein encoded has engineered N- and C-terminal polyhistidine (HIS) and influenza hemagglutinin (HA) epitope tags for antigen detection on arrays using anti-tag antibodies, and (in the case of the HIS tag) for purification by nickel chelate affinity chromatography. We wished to leverage these reagents to examine the T cell response at the VACV proteomic level, and examine the extent to which T cell and antibody profiles overlap.

We first needed a source of defined VACV-specific T cells with which to develop a proteome-wide T cell screening assay. For this we administered C57Bl/6 mice purified VACV-WR proteins in CpG/ISCOMs or alum and measured immunogenicity by conventional means, namely antibody production, and in protection assays *in vivo*. Alum is known to induce a Th2 polarized response and is a strong inducer of IgG1 in mice (33, 34), whereas CpG and ISCOMs polarize the response in a Th1 direction and induce IgG2a/c (31, 35-37). We measured IgG2c as there is a deletion of the γ2a gene in C57Bl/6 mice (38). A representative experiment is shown in Fig. 1A in which groups of 5 C57Bl/6 mice were given the purified IMV membrane protein, WR101/H3L, in either adjuvant, or in PBS as an adjuvant control. Duplicate groups of mice were administered WR101/H3L, one full length and the other deleted of the transmembrane region. This helps confirm protection was mediated by the antibody-accessible extracellular domain of the protein. Sera were obtained on d20 after a single immunization and probed against VACW-WR protein microarrays to monitor antibody production. Bound antibodies were visualized with biotinylated secondary antibodies to IgG, IgG1 and IgG2c and the average signals for each group plotted to assess the polarization of the response. The default response in the absence of adjuvant is toward IgG1 (Th2-associated), although signal intensities, which are a measure of Ig titer, were low. When an adjuvant was used signals increased: with alum a IgG1 response dominated, whereas CpG/ISCOMs engendered a more dominant IgG2c (Th1-associated) response. Array signal intensities were elevated further after boosting on day 14 (not shown) although there is significant detection of anti-epitope tags at this time. Shown in Fig. 1B are the relative proportions of the IgG1 and IgG2c signals, clearing showing the polarizing effect of the two adjuvants.

We then tested the ability of adjuvanted proteins to protect mice against an intranasal (i.n.) challenge of VACV-WR, as additional indicator of the immunogenicity of individual proteins. Our first experiments were conducted with WR101/H3L, which was shown previously to be protective when administered in Ribi or Complete Freund's adjuvants (39). We extended this observation here using CpG/ISCOMs and alum as adjuvants. After two immunizations spaced 14 days apart, the mice were challenged by the i.n. route with a sub-

lethal dose of VACV-WR. The results shown in Fig. 1C show that mice give antigen in PBS or in alum showed the most pathology, indicated by greatest weight loss and delayed onset of weight recovery. In contrast CpG/ISCOM adjuvant provided partial protection as seen by reduced weight loss and quicker onset of weight recovery. Sera taken from these mice prior to challenge showed the expected polarization of IgG1 and IgG2c as expected (data not shown). Since the arrays had serial dilutions of WR101/H3L printed, the lower limit of detection (or sensitivity) could be used as a measure of titer. These values for IgG2c and IgG1 were plotted against the corresponding nadir body weights; increasing IgG2c limit of detection/titer (Fig. 1D) correlated positively with nadir body weight, i.e., higher IgG2c titers were associated with less weight loss. In contrast, increasing IgG1 titers (Fig. 1E) was associated with more weight loss. Overall these data suggests a Th1-type response promotes protection against infection, whereas a Th2-type promotes infection-associated pathology.

Adjuvanted SDS-IBs are protective against VACV-WR challenge in vivo

We then extended this observation to 5 additional VACV-WR antigens that had been purified previously for the development of ELISA assays to monitor antibodies in DryVax® vaccinees (27). These antigens comprised WR113/D8L, which was purified from the soluble fraction of *E. coli* lysates on nickel columns, and WR148/−, WR118/D13L, WR132/A13L and WR070/I1L, which were all purified as SDS-solubilized inclusion bodies (SDS-IBs) using a generic protocol. For the latter, free SDS was removed by precipitation as described in the Materials and Methods before use *in vivo*, or with cellular assays *in vitro* (see below). An ‘empty vector’ (EV) IB preparation was prepared as negative control antigen, which consisted of material extracted from *E. coli* BL21 cells transformed with non-recombinant expression plasmid and processed in the same way as cells with inclusion bodies. Endotoxin content of all purified protein preparations ranged from 0.1-0.3 EU/ml or below. Antigens were administered to groups of 5 B6 mice in CpG/ISCOM adjuvant, and the presence of antibodies in tail bleeds measured by protein microarray on d14 (Fig. 2A). Antigen-specific antibodies were detected by the array at this time, with the exception of those that received WR118/D13L. After challenge on d14, all of the mice receiving an i.n. challenge of VACV-WR antigens showed partial protection relative to the EV control, with variations between the antigens (Fig. 2B). The protective ranking of the antigens (with average nadir body weight for each group in parenthesis) was: WR118/D13L (99%) > WR113/D8L (93%) = WR132/A13L (93%) > WR148/−(91%) > WR070/I1L (89%) > EV (~75%). Interestingly, despite being unable to detect IgG in those receiving WR118/D13L (at least by array on d14), these mice showed greatest protection from VACV-WR challenge. Of the 5 EV control mice, two mice fell to 75% of original body weight and were euthanized, while the remaining 3 mice gradually recovered. In a separate challenge experiment (Fig. 2C) four ‘irrelevant’ control proteins from *Brucella melitensis* (40) were expressed as IBs and purified using the generic SDS-solubilization method and administered in CpG/ISCOMs. After VACV-WR challenge, changes in body weights were very similar to the mice receiving EV control antigen, whereas mice receiving positive control VACV-WR antigens were protected as before. Overall, these data indicate adjuvanted SDS-IBs made in *E. coli* were non-toxic and immunogenic in mice, as demonstrated by specific-antibody production and/or protection against live i.n. VACV-WR challenge. These proteins and immunization

regimens were then used in subsequent experiments as reagents to develop a proteome-wide T cell screen.

SDS-IBs are compatible with IFN-γ release assay in vitro

Having established above that SDS-IBs were immunogenic *in vivo*, we evaluated their utility for measuring T cell responses *in vitro*. In pilot experiments, survivors of challenge experiments were euthanized, and splenocytes and cells from lymph nodes draining the nasal sinuses were subjected to IFN-γ ELISPOTs against titrations of the 5 VACV-WR and EV antigen preparations, and the same proteins expressed as IVTT reactions in 'capture' ELISPOTs. Experiments using lymph node cells and splenocytes from the survivors of the experiment shown in Fig. 2 are provided in Fig. S1. A capture ELISpot format, in which proteins expressed in IVTT were captured using immobilized anti-poly histidine tag antibody, was tested initially for HT T cell screening. However, we were unable to develop a reliable method for confirming the capture of antigen. For this reason we elected to switch to solubilized SDS-IBs as antigens which were simply added to the ELISpot without capture. Other pilot experiments showed that erythrocyte-depleted splenocytes provided optimal antigen specificity and lowest backgrounds. In addition to antigen-specific release of IFN-γ, the numbers of spot-forming cells was dose-dependent and titrated with antigen concentration in the assay. These observations strongly indicate the release was T cell rather than NK cell-mediated.

To scale the format to the whole VACV-WR proteome, the VACV-WR expression library was first transformed into *E. coli* BL21 cells, and master cell banks established as glycerol stocks in 96 well plates. We then miniaturized the generic IB purification and SDS-solubilization method used previously for larger protein preps shown in Figs. 1 and 2 to a 96-well HT format as described in the Materials and Methods. We found all of the VACV-WR proteins were solublized in 0.2% SDS when processed in the 96 well format. After removal of free SDS, a presence of soluble protein in each well was verified by printing a sample of each on microarrays and probing with antibodies to the HIS and HA tags. A heat map of the raw signals from a representative SDS-IB batch is shown in Fig. S2. In the example shown, a total of 215 (95.6%) of the vaccinia ORFs scored positive for both HIS and HA tags, with an additional 9 proteins being positive for the HA tag only. Only one protein (0.4%) out of the whole library of 225 was double negative. These numbers are consistent with VACV-WR ORF expression in IVTT reactions (41). Detection of the C-terminal HA tag is an indicator of full length protein (data not shown). The innovation of combining autoinduction with a generic IB extraction and solubilization protocol is readily scalable to much larger pathogens. The mitogenic effect of all IB preparations was also assessed in IFN-γ ELISPOTs with naïve mouse splenocytes. At a dilution of 1/10 the IB preps resulted in IFN-γ secreting cells (ISCs) per 10^6 splenocytes ranging from 0-80. This 'baseline' of ISC count was comparable to the values obtained with empty vector control preps (i.e., extracts from *E. coli* transformed with non-recombinant plasmids), and was significantly lower than the values obtained with IVTT reactions added to naïve splenocytes.

We then evaluated the soluble VACV-WR proteome first by screening splenocytes from the survivors of the challenge experiments shown in Fig. 2A and B. Shown in Fig. 3 are

splenocytes from five mice in each VACV-WR vaccine group pooled and assayed directly in 96-well IFN-γ ELISPOTs against the SDS-IB library, one protein per well at 1/20 final dilution. Splenocytes from naïve/non-challenged mice were used as controls. In each case, vaccinated mice show a dominant response to the immunizing antigen, ranging from ~900-2000 IFN-γ spot forming cells (SFCs) per 10^6 over a 'background' (~200 SFCs/10^6). Antigen-specific responses were several-fold higher than the background reactivity of the control mice. In some cases we saw a few additional subdominant 'hits' in the challenged mice which we attribute to the VACV-WR challenge itself. This modest number of subdominant hits, and variability between mice (compare panels A, C with B, D) is consistent with the infection, here delivered by a single i.n. challenge, engendering a T cell response that is at or near the threshold of detection by the assay. Overall, these data indicated that the SDS-IB library, despite the use of SDS in its production, was compatible with T cell viability and demonstrated its potential for proteome-wide screening in infected mice.

Proteome-wide T cell screening in VACV-WR infection

A primary aim of this study was to be able to assay T cells directly from VACV-WR infected mice without any prior expansion *in vitro*. For this, intraperitoneal (i.p.) administration was the preferred route of entry. Although no outwardly visible pathology or weight loss is seen in response to i.p. inoculation, these animals display splenomegaly and are completely protected from subsequent i.n. challenge (which in effect is a 'boost' of VACV-WR). The i.p. route thus offers the opportunity for higher pfu doses than would be possible via the i.n. route, and for repeat/booster exposures. Pilot studies showed single i.p. inoculums of VACV-WR engendered only weak 'hits' in the IFN-γ ELISPOT with SFC numbers close to the baseline obtained from uninfected mice, whereas mice primed i.p. and boosted by i.n. challenge demonstrated more robust responses in the IFN-γ ELISPOT that were both antigen-specific and dose-dependent (Fig. S3). This is consistent with earlier findings using individual protein immunizations (Fig. S1). One indicator to the reliability of the T cell antigen discovery methodology is consistency of responses between independent experiments in inbred mice. Shown in Fig. 4A-C are three independent proteome-wide screens from pooled spleen cell populations harvested at three different time-points after challenge (d8, d13 and d20). Overall the numbers of antigen hits and the numbers of spot forming cells per hit were similar on d8 and d13 post challenge, although these values were clearly declining by d20. The consistency between experiments was assessed by pair-wise comparisons and regression analysis (Fig. 4E-G). The highest correlation was seen between the two earlier time points, d8 and d13 (Fig. 4E), which fell slightly when compared to the latest time point, d20 (Fig. 4G).

Although no attempt was made to use purified T cell subsets in this study, the delivery of soluble (exogenous) antigens in the assay would be expected to favor stimulation of CD4 T cells rather than CD8. We therefore assayed the supernatants of ELISpot assays for signature cytokines of Th1 (IFNγ and IL2) and Th2 (IL4 and IL5) subsets (Fig. 5). Several antigens elicited the production of IFNγ and/or IL2 (Figs. 5A and B), while there was negligible detection of IL4, and low to baseline levels of IL5 (Figs. 5C and D), consistent with polarization of the CD4 response in a Th1 direction. Shown in Fig. 5E is a comparison

of the two different IFNγ assays performed on the same experiment. The ELISpot revealed a profile of 35 antigen 'hits', while the Luminex assay revealed 48 antigens, with an overlap of 24 antigens in common to both assays ($p=4.24 \times 10^{-11}$). The antigens defined by these two different IFNγ assays are listed in Table 1. Any differences between supernatant assays and cellular spot assays for T cells may simply reflect the nature of the assay. Thus it is likely that a few cells producing a lot of cytokine would score high by supernatant assays and low by ELISpot, while many cells producing a little cytokine would show the reverse.

Since Th1 cells release both IFNγ and IL2, we also compared the antigen profiles for these two cytokines (Fig. 5F). Overall, 62 antigens were positive in the IL2 assay, of which 35 were also positive in the IFNγ assay ($p=1.20 \times 10^{-13}$). These antigens are listed in Table 2. There were also 13 antigens that were positive in the IFNγ assay but negative in the IL2 assay which could potentially represent CD8 responses (indicated by the asterisks in Table 1). Comparison of these with known VACV WR-specific CD8 epitopes recognized by C57Bl/6 mice (42) indicate three of the 13 (WR149\A26L, WR125\A6L and WR008\C19L) may contain minor CD8 epitopes (see Discussion).

Comparison of antigens recognized by T cells and antibodies

The cognate antigen recognition model of T cell help for antibody predicts overlap between the antigens recognized by T cells and antibodies. To test this, sera were obtained from 8 mice administered VACV-WR i.p. (1E+5) on d0, challenged by the i.n. route (2E+6) on d13, and sacrificed on d21 for serum collection. Prior inoculation via the i.p. route completely protected the mice from weight loss after challenge via the pathogenic i.n. route (data not shown). Sera collected from the survivors were then probed against VACV-WR proteome microarrays and bound IgG determined by indirect immunofluorescence. The seroreactive antigens are listed in Table 3. Consistent with our previous protein array studies (29, 39, 41, 43) antibody profiles of VACV WR-infected mice were heavily weighted toward the recognition of late, structural proteins. Thus, of the 27 different antigens scored as seropositive, 22 (82%) were classified (32) as 'virion associated', over half of which were membrane proteins. The array signals for each antigen of the antibody profile were then plotted against the corresponding IFN-γ SFCs/10^6 of a representative ELISPOT (Fig. 6A). The temporal expression designations for each protein, defined by Yang and colleagues from deep sequencing studies (32) as early subcluster 1 (E1.1), early subcluster 2 (E1.2) and post-replicative (PR), are represented by different symbols. The overlap antigens are represented in the upper right quadrant, defined as being above the cutoff in both the antibody and T cell assays. These are overwhelmingly virion associated and comprised mostly membrane proteins. There were also antigens that appeared to be recognized by T cells only, and by antibodies only, as seen in the lower right and upper left quadrants, respectively. These differences are more clearly seen in the bar chart shown in Fig. 6B, where the signal intensities (IgG) and spots/well (T cells) are overlaid on the list of antigens comprising the whole proteome. The combined IgG and Th1 immunoproteome comprises approximately 25% of the whole proteome.

We then asked whether the antigens that comprise the immunoproteome differed significantly from the whole proteome itself. The pie charts in Fig. 6C show the proportion

of 7 different functional categories of VACV proteins (32) in the T cell and antibody profiles compared to the whole proteome. The IgG profile can be seen to be enriched for proteins with virion association, as reported previously (25). In contrast, the proportions of the 7 functional categories in the T cell profiles do not show the same degree of skewing to virion association as seen with IgG, but are more similar to the proteome itself, regardless of which IFNγ assay is used.

Comparison of antigens recognized by CD4 T cells and antibodies in response to inactivated VACV-WR

The foregoing indicates that in VACV-WR infection, antibody targets were enriched for late, virion associated proteins, while T cell antigens (thought to be Th1 CD4 cells) showed a non-biased distribution of both early and late gene products. To test the validity of this observation, we hypothesized that the T cell profile in response to heat-inactivated VACV-WR would be skewed toward virion components, and skewed away from early and early/late antigens that require expression in infected cells. By IFNγ ELISPOTs we were unable to detect a robust T cell response on d10 (Fig. 7A) although strong hits were seen after boosting by intranasal challenge (Fig. 7B). The T cell antigen profile after prime-boost comprised 17 antigens above the cut-off. Although smaller than seen with viable VACV-WR infection, these comprised 12 proteins (70%) that were virion associated (Table 4). Nine of these viron antigens were identified previously in IFNγ assays after VACV-WR infection (indicated in Table 4 by *), with the remaining 3 identified in the IL2 assay. The remaining non-virion associated proteins may represent early gene products expressed after the i.n. challenge. Sera from the same mice after prime-boost were also probed on proteome microarrays (Table 5). Pie charts of the T and antibody target antigens classified into functional categories are shown in Fig. 7C. Overall the data indicate a prime-boost is required to see a T cell response to heat-inactivated VACV-WR by IFNγ ELISPOT. Moreover, unlike the T cell profile engendered after viable VACV-WR infection (Fig. 6), the profile in response to inactivated virus is heavily skewed toward late proteins as predicted. In contrast with T cells, the proportion of IgG targets with virion association is essentially the same regardless of whether viable or inactivated VACV-WR is used as the priming antigen.

Discussion

Vaccinia virus (VACV) was used to eradicate smallpox over four decades ago, but the virus still represents an important tool for understanding vaccine-mediated adaptive immunity. There is now a considerable understanding of the importance of antibody in immunity generated by VACV. For example, depletion of B cells but not CD4 or CD8 T cells abolished VACV-mediated protection of macaques against monkeypox challenge (44). In the same study, passive transfer of human VACV-neutralizing antibodies conferred protection against challenge. Similarly, ectromelia virus (an othropoxvirus that causes mousepox) is lethal in B cell deficient mice despite mounting a CD8 T cell response, while passive transfer of immune serum allows such mice to clear an established infection and fully recover (45). The expectation that antibodies to VACV membrane proteins could mediate protection has been confirmed by virus neutralizing studies *in vitro* (39, 46-62), and

several purified membrane proteins, including WR101/H3L (39), WR187/B5R (51), WR156/A33R (51, 63, 64), WR151/A28L (59), WR132/A13L (60), and WR150/A27L (65) have been shown to protect animals against challenge *in vivo*. Proteome-wide screening by microarray for antibody targets in sera confirmed the response is heavily skewed towards recognition of virion-associated targets (29, 39, 41, 66). Unexpectedly, human antibody profiles show significant inter-individual heterogeneity (41) although a 'core' set of commonly recognized antigens is preserved. Subsequent depletion studies suggest the VACV-neutralizing activity in human serum is not mediated by antibodies to a dominant antigen in particular but by a mixture of antibodies to different antigens, each of which appears redundant in the overall response (67).

In contrast to antibodies, discovery of T cell antigens has lagged behind that of antibodies, and a full picture of the VACV immunome remains incomplete. A bottleneck traditionally has been the availability of a large number of proteins in sufficient purity to be compatible with T cell viability *in vitro* (68, 69). Cell-free IVTT reactions based on *E. coli* lysates express protein at high level and allow the production of large numbers of different proteins simultaneously. A particular advantage of this system is the antigens are expressed and maintained in soluble form in the lysate. This platform also represents a convenient way to leverage ORFeome libraries. A disadvantage that needs to be overcome is the mitogenicity of *E. coli* lysate in conventional T cell assays. Purification from IVTT is possible, although such manipulations require customization for each protein (i.e., are often not high throughput), and often cause protein insolubility issues. Jing and colleagues have obviated purification by using whole IVTT diluted to sub-mitogenic levels for T cell assay (15, 16). This also dilutes the expressed antigen, thus prior expansion of antigen-specific cells *ex vivo* is required. For this, live VACV or (more usually) UV-inactivated virus, was used as sources of restimulating antigen to generate bulk lines. Both studies report an enrichment of proteins with virion association and CD4 recognition. Thus, in a panel of 11 vaccinees, proliferative responses were detected to 122 ORFs (68%) overall, although just 6 proteins (122/A3L, 129/A10L, 118/D13L, 101/H3L, 091/L4R and WR148/−) dominated the profiles. Of these, all except 101/H3L were identified in the current mouse study as T cell antigens in C57Bl/6 mice (Table 1).

In addition to IVTT, synthetic peptides have also been used to identify T cell antigens in DryVax® vaccinees or VACV-WR infected mice. Moutaftsi and colleagues (70) synthesized 2,146 peptides (representing 30.4% of predicted VACV transcribed sequences) of which 14 peptides from 13 different antigens were recognized in IFNγ release assays by CD4 T cells from infected C57Bl/6 mice. Of the 13 recognized antigens, at least 6 (46%) were virion-associated, compared to 27% in the whole proteome (classification based on Yang et al (32)). The reason for the enrichment of virion proteins was hypothesized to be due to the preference by CD4 cells of for recognition of exogenously derived antigen (i.e, virus particles) which is taken up, processed and presented in the context of class II MHC by professional APCs. Subsequent alignment of the T cell antigens with known antibody targets showed the 6 T cell antigens that were virion associated were also known antibody targets (71). Indeed, the overlap between the CD4 antigens and antibodies was so close, that antibodies could be used to predict new T cell antigens that had not been discovered using

the peptide library (26, 71). This latter study is of particular relevance as the same mouse strain (C57Bl/6) was used here. By Luminex, 20/48 (41.7%) and by ELISpot 13/35 (37.1%) antigens were virion associated (Table 1). These proportions are slightly smaller than reported by Moutaftsi et al (70), although in both studies virion associated proteins represents the largest functional category of antigens recognized. Of the 13 antigens reported by Moutaftsi et al, 8 were also recognized in the present study (highlighted in Table 1). Any differences between the antigens discovered in the two studies are likely to reflect differences in assay systems, such as scope of the proteome covered and T cell restimulation methods used.

Calvo-Calle et al (72) used a predictive algorithm to identify putative HLA-DR1 restricted CD4 T cell epitopes in the attenuated VACV vaccine strain modified virus Ankara (MVA), and synthesized 36 candidate epitopes as peptides. T cells were first expanded *in vitro* with infected cell lysates virus. This would be expected to provide restimulatory antigens of both virion and infected cell origin (i.e., less 'biased' than inactivated virions, for example). The authors report 25 peptides recognized by vaccinated individuals, of which 9 (36%) were virion associated, compared to 27% in the proteome. Along similar lines, Moise et al (73) used a bioinformatic approach to identify MHC class I and II-restricted epitopes conserved between VACV and VARV. Candidate peptides were then screened in HLA-binding assays and also in ex-vivo cultures with PBMCs from DryVax vaccines. By this approach, 50 conserved class II-restricted peptides were identified, corresponding to 37 different VACV proteins. Of these, 32 (>86%) were reactive in IFNγ ELISpots, of which 7 (21.9%) were virion associated (according to the classification of Yang et al (32)). The largest category was 'transcription' with 14 (43.8%). In this study, CD4 antigens with virion associated are under-represented relative to the proteome, although this may simply reflect the bias of the input peptides selected for further study.

Overall, as the preceding shows, there is general agreement that CD4 T cell antigens are enriched for virion-associated proteins relative to the VACV proteome, but significantly less than the antibody profile. The extent of the enrichment in the T cell profile between different studies is likely to depend on differences between experimental protocols. Bias may be introduced by screening partial proteomes or by prior expansion of T cells with VACV antigen *in vitro*. A more divergent profile of T cell antigens compared to antibodies is consistent with the functional heterogeneity and plasticity of CD4 T cells (74-77) and the notion that only some of the responding CD4 cells measured are dependent on cognate linkage to antibody-producing B cells (see below). Although we used whole splenocytes in place of purified CD4 T cells in our assays, the delivery of exogenous antigen, and the detection of Th1-associated cytokine profile, are consistent with detection of CD4 T cell responses. Moreover, of 13 potential CD8 antigens, i.e., those that elicited IFNγ but not IL2 (indicated by asterisks in Table 1), only three (WR149\A26L, WR125\A6L and WR008\C19L) contain epitopes among the 49 CD8 epitopes recognized by ~95% of the repertoire of VACV-WR specific CD8 cells in C57Bl/6 mice (42). The 3 epitopes were ranked only 12th, 18th and 46th out of 49. Noticeably absent from our T cell responses were VACWR190/B8R and WR173/A47L which contain the most dominant CD8 epitopes (42, 78, 79).

These findings, and the fact that the presence of a CD8 epitope does not rule out a CD4 response to the antigen (as any given antigen may have both CD4 and CD8 epitopes), indicate that CD8 responses are unlikely to represent a significant component, if any, of the antigen profile reported here.

The cognate-linkage model of antigen recognition underlies the recognition of common antigens by CD4 T cells and antibody. This long-standing model, which states B cell and helper T cell epitopes need to be located on the same antigen for antibody production to occur (so-called intramolecular help), has its origins in the hapten-carrier experiments of the 1960's and 70's (80-82). The model was revised to account for help provided by epitopes on different antigens that are physically linked within the same macromolecular complex, such as a virus particle (intermolecular help). Following on from the Moutaftsi study (70), mice were immunized with individual peptides corresponding to CD4 epitopes and then infected with VACV, and the antibody profile examined by protein microarrays (71). In each case, peptide priming cause the antibody response to be directed exclusively to the antigen from which the helper epitope was derived, and not transferred to other proteins present in the virus particle. These findings are consistent with the unit of B cell-T cell help in VACV residing at the level of the individual viral protein. The authors did not rule out intermolecular help but postulated a hierarchy of physical associations between different antigens, depending on whether they remain associated or become disassociated during endocytic uptake of virions by APCs (71). In another recent study, antibody and CD4+ T cell responses to four well-characterized VACV membrane proteins were studied in a large cohort of human Dryvax® vaccinees (83). The authors reported only modest overlap between the profiles, which supported a more intermolecular model for T cell help.

This study has also identified novel T cell antigens that would not have been predicted by serology. For example, WR200/B19R, a secreted IFNα/β receptor-like glycoprotein, and the WR058/E2L hypothetical protein, were consistently recognized in both IFNγ assays and IL2 assays, but showed no detectable IgG response. Such antigens are likely recognized by T cell subsets that are not cognately linked to an antibody producing B cell. Reciprocally, there are antigens that are consistent inducers of antibody but which failed to elicit a measurable T cell response (at least in the assays used here). Most notable in this category is WR101/H3L, which is a dominant specificity of the IgG profile in response to infection in both mice and humans and a protective antigen in mouse challenge studies (39). Despite this, WR101/H3L was not a strong inducer of IFNγ (in either the ELISpot or Luminex® assay) or IL2, falling just below the cut-off in each case (Figs. 5, 6). This is unlikely to be a problem of the antigen used for T cell screening, since it was detected by anti-epitope tag antibodies during QC (Fig. S2). Additional studies with T cell assays at different time points after infection, or using different cytokines may help to resolve such questions.

In addition to addressing interesting immunological questions, the ability to identify T cell and antibody targets within proteome screens of pathogens has practical applications. For example, antigens that score strongly in both the T cell and antibody screens might be considered higher priority candidates for subunit vaccines than antigens discovered by either screen alone. We have also identified new potential subunit vaccine antigens in the course of this study (Fig. 2). To our knowledge this is the first time that protection has been

engendered against the virion associated proteins WR148/−, WR118/D13L, and WR070/I1L. These antigens were selected based on their dominance among the antibody profile in mice and humans. Since none are membrane proteins, protection against pathogenic VACV challenge was not anticipated. In these cases, protection may be mediated entirely T cell mediated, although further studies will be needed to understand their mode of protection more precisely.

Supplementary Material

Refer to Web version on PubMed Central for supplementary material.

Acknowledgments

We thank Douglas Molina, Andy Teng and the microarray printing team at Antigen Discovery Inc., for producing the VACV-WR proteome arrays used in this study.

References

1. De Groot AS. Immunome-derived vaccines. Expert Opin Biol Ther. 2004; 4:767–772. [PubMed: 15174960]
2. Doolan DL. Plasmodium immunomics. Int J Parasitol. 2011; 41:3–20. [PubMed: 20816843]
3. Bagnoli F, Baudner B, Mishra RP, Bartolini E, Fiaschi L, Mariotti P, Nardi-Dei V, Boucher P, Rappuoli R. Designing the next generation of vaccines for global public health. Omics : a journal of integrative biology. 2011; 15:545–566. [PubMed: 21682594]
4. Townsend AR, Rothbard J, Gotch FM, Bahadur G, Wraith D, McMichael AJ. The epitopes of influenza nucleoprotein recognized by cytotoxic T lymphocytes can be defined with short synthetic peptides. Cell. 1986; 44:959–968. [PubMed: 2420472]
5. Lundegaard C, Lund O, Buus S, Nielsen M. Major histocompatibility complex class I binding predictions as a tool in epitope discovery. Immunology. 2010; 130:309–318. [PubMed: 20518827]
6. Stern LJ, Calvo-Calle JM. HLA-DR: molecular insights and vaccine design. Curr Pharm Des. 2009; 15:3249–3261. [PubMed: 19860674]
7. Kim Y, Sette A, Peters B. Applications for T-cell epitope queries and tools in the Immune Epitope Database and Analysis Resource. J Immunol Methods. 2010
8. Vita R, Peters B, Josephs Z, de Matos P, Ennis M, Turner S, Steinbeck C, Seymour E, Zarebski L, Sette A. A Model for Collaborative Curation, The IEDB and ChEBI Curation of Non-peptidic Epitopes. Immunome Res. 2011; 7:1–8.
9. Vita R, Zarebski L, Greenbaum JA, Emami H, Hoof I, Salimi N, Damle R, Sette A, Peters B. The immune epitope database 2.0. Nucleic Acids Res. 2009; 38:D854–862. [PubMed: 19906713]
10. Purcell AW, Gorman JJ. Immunoproteomics: Mass spectrometry-based methods to study the targets of the immune response. Mol Cell Proteomics. 2004; 3:193–208. [PubMed: 14718575]
11. Hillen N, Stevanovic S. Contribution of mass spectrometry-based proteomics to immunology. Expert Rev Proteomics. 2006; 3:653–664. [PubMed: 17181480]
12. Karunakaran KP, Yu H, Foster LJ, Brunham RC. Development of a Chlamydia trachomatis T cell Vaccine. Hum Vaccin. 2010; 6:676–680. [PubMed: 20523121]
13. Hunt DF, Henderson RA, Shabanowitz J, Sakaguchi K, Michel H, Sevilir N, Cox AL, Appella E, Engelhard VH. Characterization of peptides bound to the class I MHC molecule HLA-A2.1 by mass spectrometry. Science. 1992; 255:1261–1263. [PubMed: 1546328]
14. Johnson KL, Ovsyannikova IG, Mason CJ, Bergen HR 3rd, Poland GA. Discovery of naturally processed and HLA-presented class I peptides from vaccinia virus infection using mass spectrometry for vaccine development. Vaccine. 2009; 28:38–47. [PubMed: 19822231]

15. Jing L, Davies DH, Chong TM, Chun S, McClurkan CL, Huang J, Story BT, Molina DM, Hirst S, Felgner PL, Koelle DM. An extremely diverse CD4 response to vaccinia virus in humans is revealed by proteome-wide T cell profiling. J Virol. 2008 PMID18480455.
16. Jing L, McCaughey SM, Davies DH, Chong TM, Felgner PL, De Rosa SC, Wilson CB, Koelle DM. ORFeome approach to the clonal, HLA allele-specific CD4 T-cell response to a complex pathogen in humans. J Immunol Methods. 2009; 347:36–45. PMID 19520082. [PubMed: 19520082]
17. Moffitt KL, Gierahn TM, Lu YJ, Gouveia P, Alderson M, Flechtner JB, Higgins DE, Malley R. T(H)17-based vaccine design for prevention of Streptococcus pneumoniae colonization. Cell Host Microbe. 2011; 9:158–165. [PubMed: 21320698]
18. Turner MJ, Abdul-Alim CS, Willis RA, Fisher TL, Lord EM, Frelinger JG. T-cell antigen discovery (T-CAD) assay: a novel technique for identifying T cell epitopes. J Immunol Methods. 2001; 256:107–119. [PubMed: 11516759]
19. Valentino M, Frelinger J. An approach to the identification of T cell epitopes in the genomic era: application to Francisella tularensis. Immunol Res. 2009
20. Valentino MD, Maben ZJ, Hensley LL, Woolard MD, Kawula TH, Frelinger JA, Frelinger JG. Identification of T-cell epitopes in Francisella tularensis using an ordered protein array of serological targets. Immunology. 2011; 132:348–360. [PubMed: 21214540]
21. Valentino MD, Abdul-Alim CS, Maben ZJ, Skrombolas D, Hensley LL, Kawula TH, Dziejman M, Lord EM, Frelinger JA, Frelinger JG. A broadly applicable approach to T cell epitope identification: Application to improving tumor associated epitopes and identifying epitopes in complex pathogens. J Immunol Methods. 2011; 373:111–126. [PubMed: 21872603]
22. Koelle DM. Expression cloning for the discovery of viral antigens and epitopes recognized by T cells. Methods. 2003; 29:213–226. [PubMed: 12725787]
23. Koelle DM, Chen HB, Gavin MA, Wald A, Kwok WW, Corey L. CD8 CTL from genital herpes simplex lesions: recognition of viral tegument and immediate early proteins and lysis of infected cutaneous cells. J Immunol. 2001; 166:4049–4058. [PubMed: 11238653]
24. Koelle DM, Corey L. Recent progress in herpes simplex virus immunobiology and vaccine research. Clin Microbiol Rev. 2003; 16:96–113. [PubMed: 12525427]
25. Moutaftsi M, Tscharke DC, Vaughan K, Koelle DM, Stern L, Calvo-Calle M, Ennis F, Terajima M, Sutter G, Crotty S, Drexler I, Franchini G, Yewdell JW, Head SR, Blum J, Peters B, Sette A. Uncovering the interplay between CD8, CD4 and antibody responses to complex pathogens. Future Microbiol. 2010; 5:221–239. [PubMed: 20143946]
26. Sette A, Grey H, Oseroff C, Peters B, Moutaftsi M, Crotty S, Assarsson E, Greenbaum J, Kim Y, Kolla R, Tscharke D, Koelle D, Johnson RP, Blum J, Head S, Sidney J. Definition of epitopes and antigens recognized by vaccinia specific immune responses: their conservation in variola virus sequences, and use as a model system to study complex pathogens. Vaccine. 2009; 27(Suppl 6):G21–26. [PubMed: 20006135]
27. Hermanson G, Chun S, Felgner J, Tan X, Pablo J, Nakajima-Sasaki R, Molina DM, Felgner PL, Liang X, Davies DH. Measurement of antibody responses to Modified Vaccinia virus Ankara (MVA) and Dryvax((R)) using proteome microarrays and development of recombinant protein ELISAs. Vaccine. 2011; 30:614–625. [PubMed: 22100890]
28. Tan X, Chun S, Pablo J, Felgner P, Liang X, Davies DH. Failure of the smallpox vaccine to develop a skin lesion in vaccinia virus-naive individuals is related to differences in antibody profiles before vaccination, not after. Clin Vaccine Immunol. 2012; 19:418–428. [PubMed: 22258709]
29. Davies DH, Liang X, Hernandez JE, Randall A, Hirst S, Mu Y, Romero KM, Nguyen TT, Kalantari-Dehaghi M, Crotty S, Baldi P, Villarreal LP, Felgner PL. Profiling the humoral immune response to infection by using proteome microarrays: high-throughput vaccine and diagnostic antigen discovery. Proc Natl Acad Sci U S A. 2005; 102:547–552. [PubMed: 15647345]
30. Doolan DL, Mu Y, Unal B, Sundaresh S, Hirst S, Valdez C, Randall A, Molina D, Liang X, Freilich DA, Oloo JA, Blair PL, Aguiar JC, Baldi P, Davies DH, Felgner PL. Profiling humoral immune responses to P. falciparum infection with protein microarrays. Proteomics. 2008; 8:4680–4694. [PubMed: 18937256]

31. Eyles JE, Unal B, Hartley MG, Newstead SL, Flick-Smith H, Prior JL, Oyston PC, Randall A, Mu Y, Hirst S, Molina DM, Davies DH, Milne T, Griffin KF, Baldi P, Titball RW, Felgner PL. Immunodominant Francisella tularensis antigens identified using proteome microarray. Proteomics. 2007; 7:2172–2183. [PubMed: 17533643]
32. Yang Z, Bruno DP, Martens CA, Porcella SF, Moss B. Simultaneous high-resolution analysis of vaccinia virus and host cell transcriptomes by deep RNA sequencing. Proc Natl Acad Sci U S A. 2010; 107:11513–11518. [PubMed: 20534518]
33. Brewer JM, Conacher M, Hunter CA, Mohrs M, Brombacher F, Alexander J. Aluminium hydroxide adjuvant initiates strong antigen-specific Th2 responses in the absence of IL-4- or IL-13-mediated signaling. J Immunol. 1999; 163:6448–6454. [PubMed: 10586035]
34. Grun JL, Maurer PH. Different T helper cell subsets elicited in mice utilizing two different adjuvant vehicles: the role of endogenous interleukin 1 in proliferative responses. Cellular immunology. 1989; 121:134–145. [PubMed: 2524278]
35. Morein F, Bengtsson KL. Functional aspects of iscoms. Immunol Cell Biol. 1998; 76:295–299. [PubMed: 9723770]
36. Chu RS, Askew D, Harding CV. CpG DNA switches on Th1 immunity and modulates antigen-presenting cell function. Current topics in microbiology and immunology. 2000; 247:199–210. [PubMed: 10689789]
37. Krieg AM. CpG motifs in bacterial DNA and their immune effects. Annu Rev Immunol. 2002; 20:709–760. [PubMed: 11861616]
38. Martin RM, Brady JL, Lew AM. The need for IgG2c specific antiserum when isotyping antibodies from C57BL/6 and NOD mice. J Immunol Methods. 1998; 212:187–192. [PubMed: 9672206]
39. Davies DH, McCausland MM, Valdez C, Huynh D, Hernandez JE, Mu Y, Hirst S, Villarreal L, Felgner PL, Crotty S. Vaccinia virus H3L envelope protein is a major target of neutralizing antibodies in humans and elicits protection against lethal challenge in mice. J Virol. 2005; 79:11724–11733. [PubMed: 16140750]
40. Liang L, Tan X, Juarez S, Villaverde H, Pablo J, Nakajima-Sasaki R, Gotuzzo E, Saito M, Hermanson G, Molina D, Felgner S, Morrow WJ, Liang X, Gilman RH, Davies DH, Tsolis RM, Vinetz JM, Felgner PL. Systems biology approach predicts antibody signature associated with Brucella melitensis infection in humans. J Proteome Res. 2011; 10:4813–4824. [PubMed: 21863892]
41. Davies DH, Molina DM, Wrammert J, Miller J, Hirst S, Mu Y, Pablo J, Unal B, Nakajima-Sasaki R, Liang X, Crotty S, Karem KL, Damon IK, Ahmed R, Villarreal L, Felgner PL. Proteome-wide analysis of the serological response to vaccinia and smallpox. Proteomics. 2007; 7:1678–1686. [PubMed: 17443847]
42. Moutaftsi M, Peters B, Pasquetto V, Tscharke DC, Sidney J, Bui HH, Grey H, Sette A. A consensus epitope prediction approach identifies the breadth of murine T(CD8+)-cell responses to vaccinia virus. Nature biotechnology. 2006; 24:817–819.
43. Davies DH, Wyatt LS, Newman FK, Earl PL, Chun S, Hernandez JE, Molina DM, Hirst S, Moss B, Frey SE, Felgner PL. Antibody profiling by proteome microarray reveals the immunogenicity of the attenuated smallpox vaccine modified vaccinia virus ankara is comparable to that of Dryvax. J Virol. 2008; 82:652–663. [PubMed: 17977963]
44. Edghill-Smith Y, Golding H, Manischewitz J, King LR, Scott D, Bray M, Nalca A, Hooper JW, Whitehouse CA, Schmitz JE, Reimann KA, Franchini G. Smallpox vaccine-induced antibodies are necessary and sufficient for protection against monkeypox virus. Nat Med. 2005; 11:740–747. [PubMed: 15951823]
45. Chaudhri G, Panchanathan V, Bluethmann H, Karupiah G. Obligatory requirement for antibody in recovery from a primary poxvirus infection. J Virol. 2006; 80:6339–6344. [PubMed: 16775322]
46. Rodriguez JF, Janeczko R, Esteban M. Isolation and characterization of neutralizing monoclonal antibodies to vaccinia virus. J Virol. 1985; 56:482–488. [PubMed: 4057358]
47. Ichihashi Y, Takahashi T, Oie M. Identification of a vaccinia virus penetration protein. Virology. 1994; 202:834–843. [PubMed: 8030246]

48. Wolffe EJ, Vijaya S, Moss B. A myristylated membrane protein encoded by the vaccinia virus L1R open reading frame is the target of potent neutralizing monoclonal antibodies. Virology. 1995; 211:53–63. [PubMed: 7645236]
49. Ichihashi Y, Oie M. Neutralizing epitope on penetration protein of vaccinia virus. Virology. 1996; 220:491–494. [PubMed: 8661400]
50. Hsiao JC, Chung CS, Chang W. Vaccinia virus envelope D8L protein binds to cell surface chondroitin sulfate and mediates the adsorption of intracellular mature virions to cells. J Virol. 1999; 73:8750–8761. [PubMed: 10482629]
51. Galmiche MC, Goenaga J, Wittek R, Rindisbacher L. Neutralizing and protective antibodies directed against vaccinia virus envelope antigens. Virology. 1999; 254:71–80. [PubMed: 9927575]
52. Wallengren K, Risco C, Krijnse-Locker J, Esteban M, Rodriguez D. The A17L gene product of vaccinia virus is exposed on the surface of IMV. Virology. 2001; 290:143–152. [PubMed: 11882999]
53. Bell E, Shamim M, Whitbeck JC, Sfyroera G, Lambris JD, Isaacs SN. Antibodies against the extracellular enveloped virus B5R protein are mainly responsible for the EEV neutralizing capacity of vaccinia immune globulin. Virology. 2004; 325:425–431. [PubMed: 15246280]
54. Putz MM, Midgley CM, Law M, Smith GL. Quantification of antibody responses against multiple antigens of the two infectious forms of Vaccinia virus provides a benchmark for smallpox vaccination. Nat Med. 2006; 12:1310–1315. [PubMed: 17086190]
55. Nelson GE, Sisler JR, Chandran D, Moss B. Vaccinia virus entry/fusion complex subunit A28 is a target of neutralizing and protective antibodies. Virology. 2008; 380:394–401. [PubMed: 18789472]
56. Benhnia MR, McCausland MM, Moyron J, Laudenslager J, Granger S, Rickert S, Koriazova L, Kubo R, Kato S, Crotty S. Vaccinia virus extracellular enveloped virion neutralization in vitro and protection in vivo depend on complement. J Virol. 2009; 83:1201–1215. [PubMed: 19019965]
57. Benhnia MR, McCausland MM, Laudenslager J, Granger SW, Rickert S, Koriazova L, Tahara T, Kubo RT, Kato S, Crotty S. Heavily isotype-dependent protective activities of human antibodies against vaccinia virus extracellular virion antigen B5. J Virol. 2009; 83:12355–12367. [PubMed: 19793826]
58. McCausland MM, Benhnia MR, Crickard L, Laudenslager J, Granger SW, Tahara T, Kubo R, Koriazova L, Kato S, Crotty S. Combination therapy of vaccinia virus infection with human anti-H3 and anti-B5 monoclonal antibodies in a small animal model. Antiviral therapy. 2010; 15:661–675. [PubMed: 20587859]
59. Shinoda K, Wyatt LS, Moss B. The neutralizing antibody response to the vaccinia virus A28 protein is specifically enhanced by its association with the H2 protein. Virology. 2010; 405:41–49. [PubMed: 20673745]
60. Xu C, Meng X, Yan B, Crotty S, Deng J, Xiang Y. An epitope conserved in orthopoxvirus A13 envelope protein is the target of neutralizing and protective antibodies. Virology. 2011; 418:67–73. [PubMed: 21810533]
61. Matho MH, Maybeno M, Benhnia MR, Becker D, Meng X, Xiang Y, Crotty S, Peters B, Zajonc DM. Structural and biochemical characterization of the vaccinia virus envelope protein D8 and its recognition by the antibody LA5. J Virol. 2012; 86:8050–8058. [PubMed: 22623786]
62. Benhnia MR, Maybeno M, Blum D, Aguilar-Sino R, Matho M, Meng X, Head S, Felgner PL, Zajonc DM, Koriazova L, Kato S, Burton DR, Xiang Y, Crowe JE Jr. Peters B, Crotty S. Unusual features of vaccinia virus extracellular virion form neutralization resistance revealed in human antibody responses to the smallpox vaccine. J Virol. 2013; 87:1569–1585. [PubMed: 23152530]
63. Paran N, Lustig S, Zvi A, Erez N, Israely T, Melamed S, Politi B, Ben-Nathan D, Schneider P, Lachmi B, Israeli O, Stein D, Levin R, Olshevsky U. Active vaccination with vaccinia virus A33 protects mice against lethal vaccinia and ectromelia viruses but not against cowpoxvirus; elucidation of the specific adaptive immune response. Virol J. 2013; 10:229. [PubMed: 23842430]
64. Fang M, Cheng H, Dai Z, Bu Z, Sigal LJ. Immunization with a single extracellular enveloped virus protein produced in bacteria provides partial protection from a lethal orthopoxvirus infection in a natural host. Virology. 2006; 345:231–243. [PubMed: 16256161]

65. Rudraraju R, Ramsay AJ. Single-shot immunization with recombinant adenovirus encoding vaccinia virus glycoprotein A27L is protective against a virulent respiratory poxvirus infection. Vaccine. 2010; 28:4997–5004. [PubMed: 20653083]
66. Schmid K, Keasey SL, Pittman P, Emerson GL, Meegan J, Tikhonov AP, Chen G, Schweitzer B, Ulrich RG. Analysis of the human immune response to vaccinia by use of a novel protein microarray suggests that antibodies recognize less than 10% of the total viral proteome. Proteomics Clin Appl. 2008; 2:1528–1538. [PubMed: 21136800]
67. Benhnia MR, McCausland MM, Su HP, Singh K, Hoffmann J, Davies DH, Felgner PL, Head S, Sette A, Garboczi DN, Crotty S. Redundancy and plasticity of neutralizing antibody responses are cornerstone attributes of the human immune response to the smallpox vaccine. J Virol. 2008; 82:3751–3768. PMID18234801. [PubMed: 18234801]
68. Grubaugh D, Flechtner JB, Higgins DE. Proteins as T cell antigens: methods for high-throughput identification. Vaccine. 2013; 31:3805–3810. [PubMed: 23806245]
69. Cardoso FC, Roddick JS, Groves P, Doolan DL. Evaluation of approaches to identify the targets of cellular immunity on a proteome-wide scale. PLoS One. 2011; 6:e27666. [PubMed: 22096610]
70. Moutaftsi M, Bui HH, Peters B, Sidney J, Salek-Ardakani S, Oseroff C, Pasquetto V, Crotty S, Croft M, Lefkowitz EJ, Grey H, Sette A. Vaccinia virus-specific CD4+ T cell responses target a set of antigens largely distinct from those targeted by CD8+ T cell responses. J Immunol. 2007; 178:6814–6820. [PubMed: 17513729]
71. Sette A, Moutaftsi M, Moyron-Quiroz J, McCausland MM, Davies DH, Johnston RJ, Peters B, Rafii-El-Idrissi Benhnia M, Hoffmann J, Su HP, Singh K, Garboczi DN, Head S, Grey H, Felgner PL, Crotty S. Selective CD4+ T cell help for antibody responses to a large viral pathogen: deterministic linkage of specificities. Immunity. 2008; 28:847–858. PMID 18549802. [PubMed: 18549802]
72. Calvo-Calle JM, Strug I, Nastke MD, Baker SP, Stern LJ. Human CD4+ T cell epitopes from vaccinia virus induced by vaccination or infection. PLoS Pathog. 2007; 3:1511–1529. [PubMed: 17937498]
73. Moise L, McMurry JA, Buus S, Frey S, Martin WD, De Groot AS. In silico-accelerated identification of conserved and immunogenic variola/vaccinia T-cell epitopes. Vaccine. 2009; 27:6471–6479. [PubMed: 19559119]
74. Sant AJ, McMichael A. Revealing the role of CD4(+) T cells in viral immunity. The Journal of experimental medicine. 2012; 209:1391–1395. [PubMed: 22851641]
75. Nakayamada S, Takahashi H, Kanno Y, O'Shea JJ. Helper T cell diversity and plasticity. Curr Opin Immunol. 2012; 24:297–302. [PubMed: 22341735]
76. Mucida D, Cheroutre H. The many face-lifts of CD4 T helper cells. Advances in immunology. 2010; 107:139–152. [PubMed: 21034973]
77. O'Shea JJ, Paul WE. Mechanisms underlying lineage commitment and plasticity of helper CD4+ T cells. Science. 2010; 327:1098–1102. [PubMed: 20185720]
78. Tscharke DC, Karupiah G, Zhou J, Palmore T, Irvine KR, Haeryfar SM, Williams S, Sidney J, Sette A, Bennink JR, Yewdell JW. Identification of poxvirus CD8+ T cell determinants to enable rational design and characterization of smallpox vaccines. The Journal of experimental medicine. 2005; 201:95–104. [PubMed: 15623576]
79. Yuen TJ, Flesch IE, Hollett NA, Dobson BM, Russell TA, Fahrer AM, Tscharke DC. Analysis of A47, an immunoprevalent protein of vaccinia virus, leads to a reevaluation of the total antiviral CD8+ T cell response. J Virol. 2010; 84:10220–10229. [PubMed: 20668091]
80. Ovary Z, Benacerraf B. Immunological Specificity of the Secondary Response with Dinitrophenylated Proteins. Proceedings of the Society for Experimental Biology and Medicine. Society for Experimental Biology and Medicine. 1963; 114:72–76.
81. Mitchison NA. The carrier effect in the secondary response to hapten-protein conjugates. II. Cellular cooperation. Eur J Immunol. 1971; 1:18–27. [PubMed: 14978857]
82. Raff MC. Role of thymus-derived lymphocytes in the secondary humoral immune response in mice. Nature. 1970; 226:1257–1258. [PubMed: 4192904]

83. Yin L, Calvo-Calle JM, Cruz J, Newman FK, Frey SE, Ennis FA, Stern LJ. CD4+ T cells provide intermolecular help to generate robust antibody responses in vaccinia virus-vaccinated humans. J Immunol. 2013; 190:6023–6033. [PubMed: 23667112]

84. Assarsson E, Greenbaum JA, Sundstrom M, Schaffer L, Hammond JA, Pasquetto V, Oseroff C, Hendrickson RC, Lefkowitz EJ, Tscharke DC, Sidney J, Grey HM, Head SR, Peters B, Sette A. Kinetic analysis of a complete poxvirus transcriptome reveals an immediate-early class of genes. Proc Natl Acad Sci U S A. 2008; 105:2140–2145. [PubMed: 18245380]

85. Rubins KH, Hensley LE, Bell GW, Wang C, Lefkowitz EJ, Brown PO, Relman DA. Comparative analysis of viral gene expression programs during poxvirus infection: a transcriptional map of the vaccinia and monkeypox genomes. PLoS One. 2008; 3:e2628. [PubMed: 18612436]

86. Resch W, Hixson KK, Moore RJ, Lipton MS, Moss B. Protein composition of the vaccinia virus mature virion. Virology. 2007; 358:233–247. [PubMed: 17005230]

87. Chung CS, Chen CH, Ho MY, Huang CY, Liao CL, Chang W. Vaccinia virus proteome: identification of proteins in vaccinia virus intracellular mature virion particles. J Virol. 2006; 80:2127–2140. [PubMed: 16474121]

88. Kunnath-Velayudhan S, Salamon H, Wang HY, Davidow AL, Molina DM, Huynh VT, Cirillo DM, Michel G, Talbot EA, Perkins MD, Felgner PL, Liang X, Gennaro ML. Dynamic antibody responses to the Mycobacterium tuberculosis proteome. Proc Natl Acad Sci U S A. 2010; 107:14703–14708. [PubMed: 20668240]

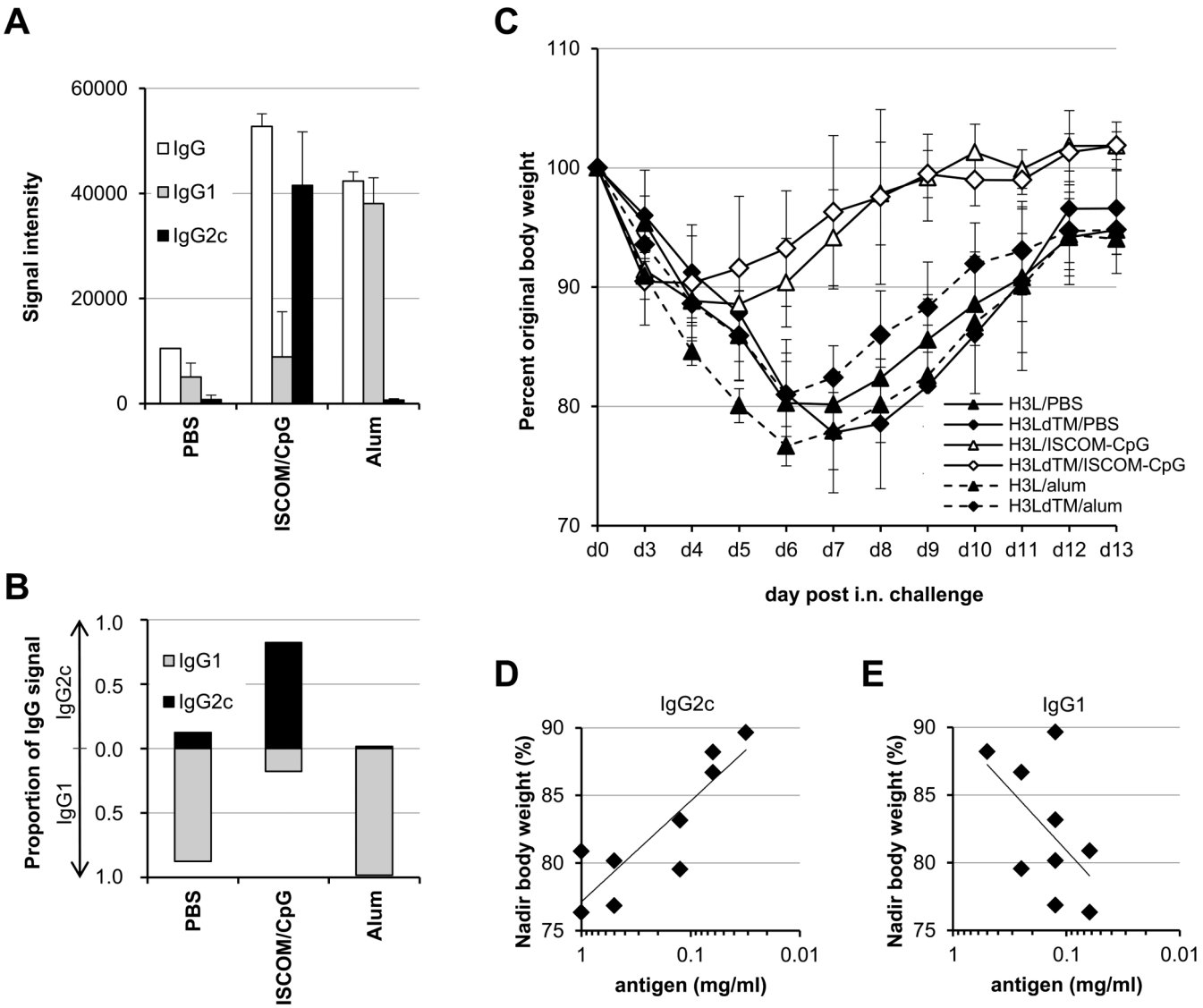

Figure 1. Immunogenicity of purified VACV-WR antigen, measured by antibody production and protection against VACV-WR challenge in mice

(A) IgG subtype analysis. Antibodies were engendered in C57Bl/6 mice against nickel column-purified VACV IMV membrane protein, WR101/H3LΔTM that has been adjuvanted in CpG/ISCOMs or alum, or in PBS alone as a control. Sera were obtained after 14 days and probed against VACV proteome microarrays on to which 8 two-fold serial dilutions of purified WR101/H3L were printed. Specific reactivity to purified WR101/H3L was visualized using fluorescently-tagged secondary antibodies to IgG, IgG1 and IgG2c and signal intensities quantified in a confocal laser scanner; data for a single concentration of printed antigen is shown. **(B)** Relative proportions of IgG1 and IgG2c derived from data shown in (A). The IgG2a proportion of the total signal is shown above the zero line, and the IgG1 proportion shown below. The IgG response is polarized according to adjuvant. **(C)** Protection of B6 mice against intranasal (i.n.) challenge of VACV-WR using adjuvanted WR101/H3LΔTM and WR101/H3L. CpG/ISCOMs reduce weight loss and promote

recovery compared to alum or PBS. **(D)** and **(E)** correlations between nadir body weight (expressed as percentage of original body weight) and titer of IgG2c and IgG1, respectively. Titer was defined from the WR101/H3L titration series on the array at the lowest concentration to give a signal intensity >2000. Liner regression was used to generate the trend lines.

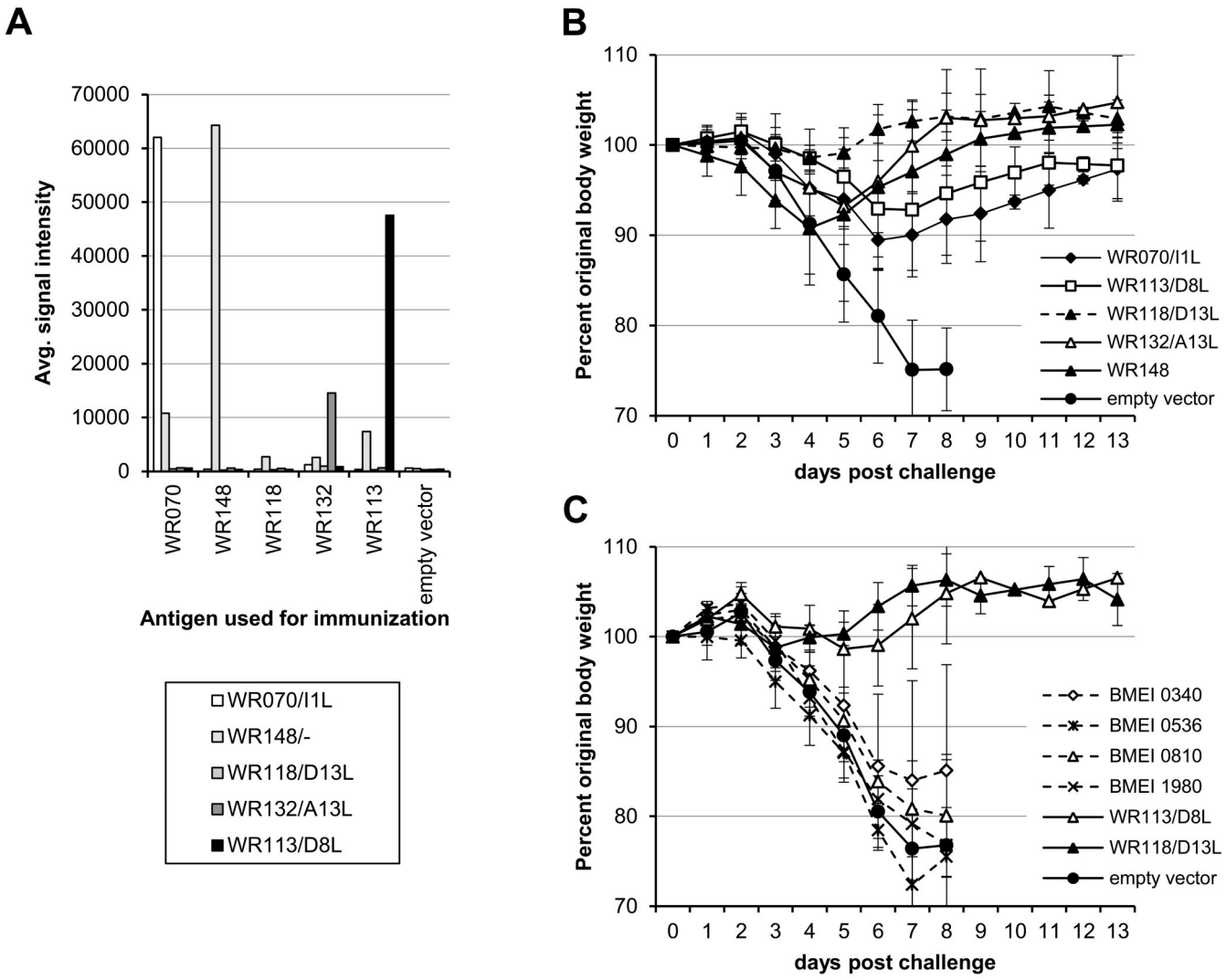

Figure 2. Immunogenicity of VACV-WR antigen purified as SDS-solubilized inclusion bodies (SDS-IBs)

Groups of five B6 mice were administered five different VACV antigens in CpG/ISCOM adjuvant. WR113/D8L was purified by conventional nickel-chelate chromatography optimized for this protein, whereas the remaining four antigens were all expressed and purified as SDS-IBs using a generic protocol. (**A**) Antibody profiles on d14 prior to VACV-WR i.n. challenge determined using VACV-WR proteome arrays. (B) Protection studies of mice against i.n. challenge of VACV-WR. (**C**) Protection studies of mice administered SDS-IBs of four different negative control antigens from *B. melitensis*, two positive control antigens from VACV-WR, or empty vector controls.

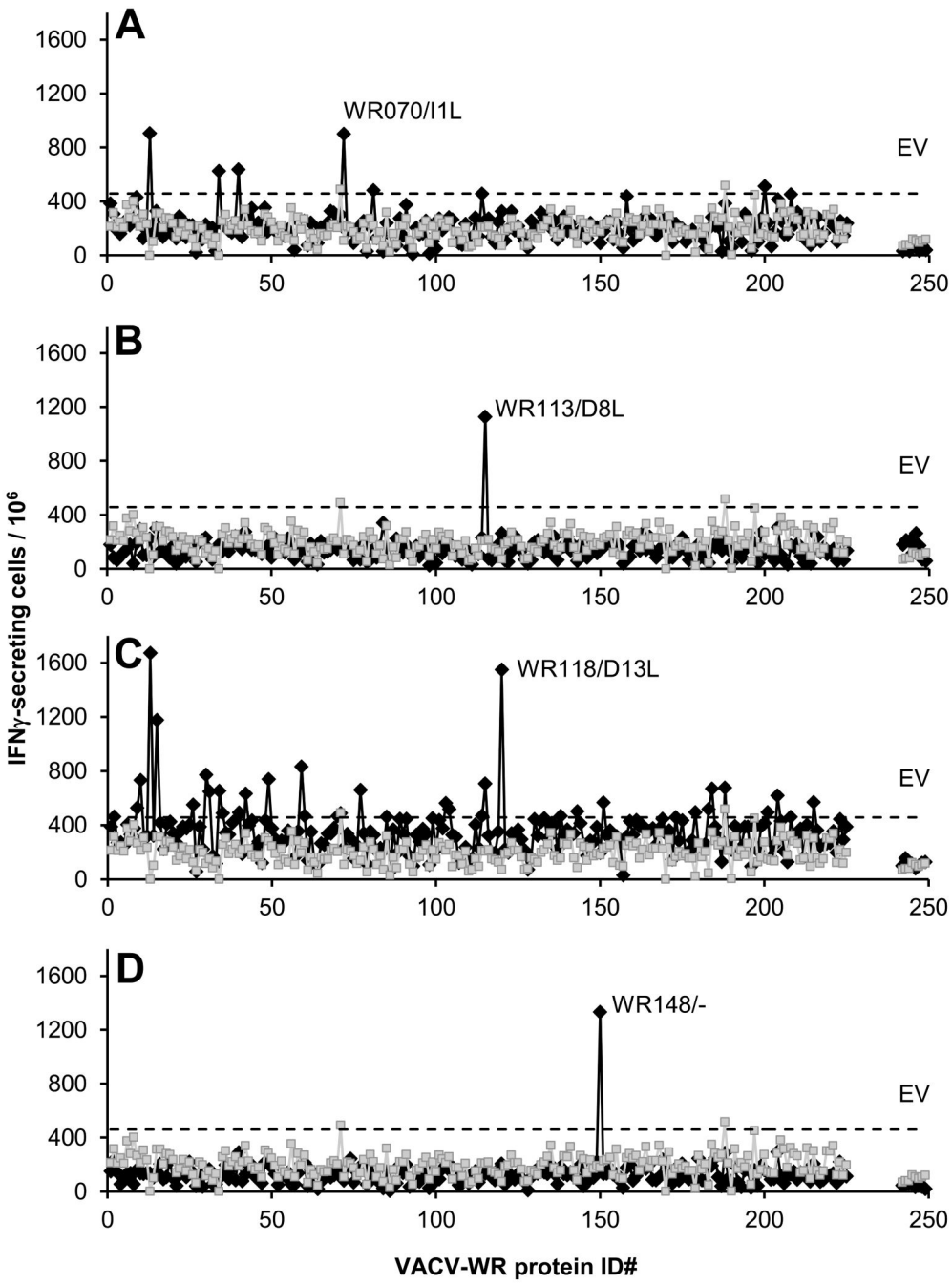

Figure 3. Verification of SDS-solubilized VACV-WR proteome for T cell screening

Spleen cells from mice administered four different individual VACV-WR proteins adjuvanted in CpG/ISCOMs and challenged with VACV-WR via i.n. route (shown in Figs. 2 and S1) were screened against the full SDS-IB VACV-WR proteome (n=220 proteins) in IFNγ ELISPOTs. Black symbols are numbers of spot-forming cells from mice administered WR070/I1L, WR113/D8L, WR118/D13L and WR148/− in CpG/ISCOM adjuvant (panels **A, B, C** and **D**, respectively). Grey symbols are responses by unimmunized/non-challenged control mice and are repeated in each panel for comparison. Eight replicate wells containing

inclusion body preps made from bacteria transformed with empty expression vector are shown, right (EV).The hashed line corresponds to the average +3SD of the response to all the antigens by the uninfected mice.

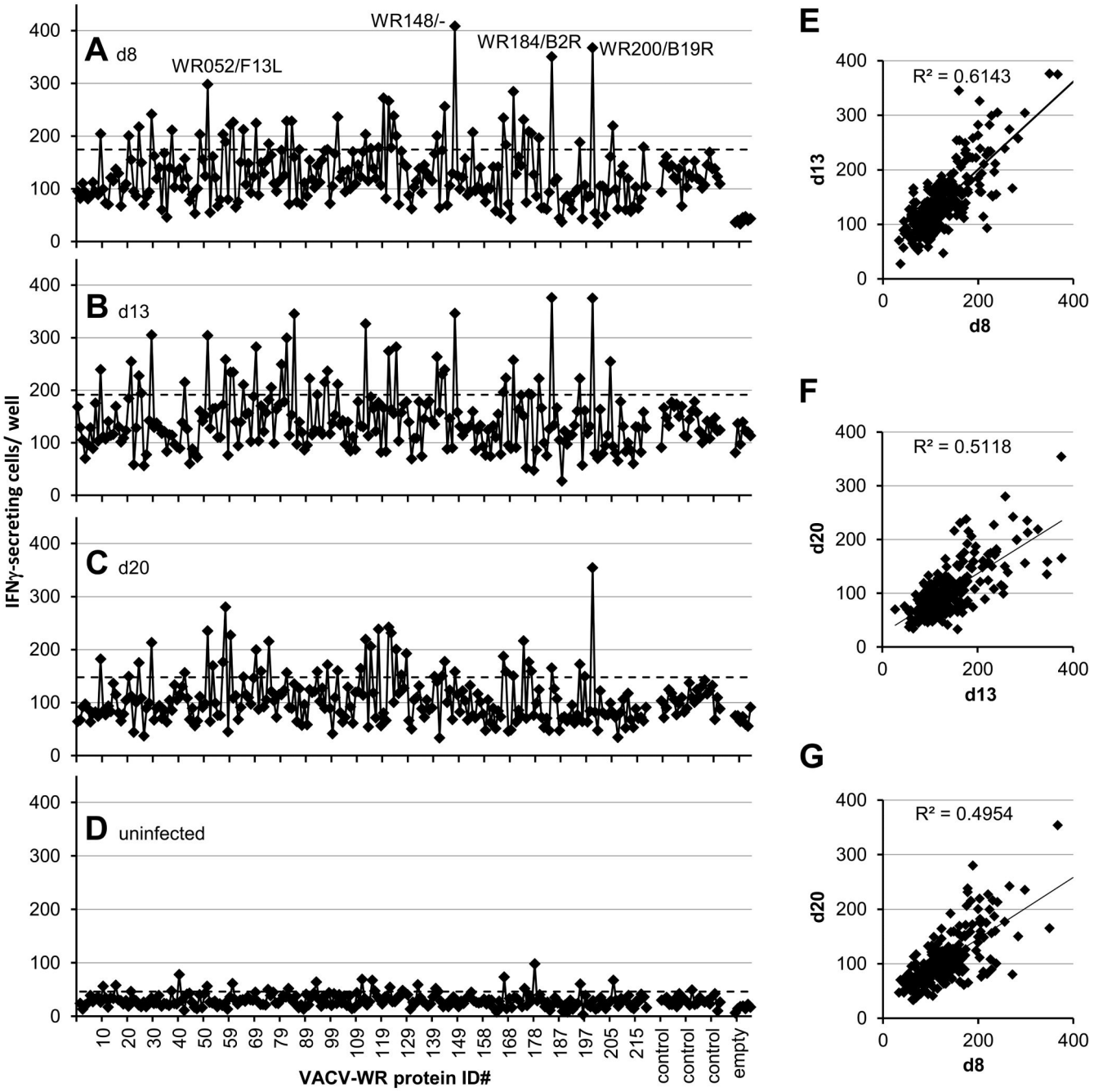

Figure 4. Proteome-wide screen of splenocytes from VACV-WR infected mice by IFNγ ELISPOT

C57Bl/6 mice were administered VACV-WR i.p. (1E+5) on d0 and challenged by the i.n. route (2E+6) on d14. No weight loss was seen during this time. Spleen cells from three mice were pooled on days 8, 13 and 20 post-challenge and subjected to screening against the full SDS-IB VACV-WR proteome (n=220 proteins) in IFN-γ ELISPOTs, at 5×10^5 cells/well (panels **A**, **B** and **C**, respectively). Four immunodominant antigens are highlighted for orientation. Cells were also screened against 24 control antigens comprising solubilized SDS-IBs produced from *Plasmodium falciparum* (30) and *Francisella tuarensis* (31)

expression libraries, and 7 empty wells that contained spleen cells with no antigens. One well contained 1μg/ml Concanavalin A as a positive control (not shown), which usually gave >600 spots/well and was defined by the plate counter software as too numerous to count. Hashed lines represent a cut-off defined as the means+2SD of the response to control antigens. **D**, uninfected mice. Pairwise comparisons of profiles were performed by scatter plots: **E**, d8 v. d13; **F**, d13 v. d20; **G**, d8 v. d20.

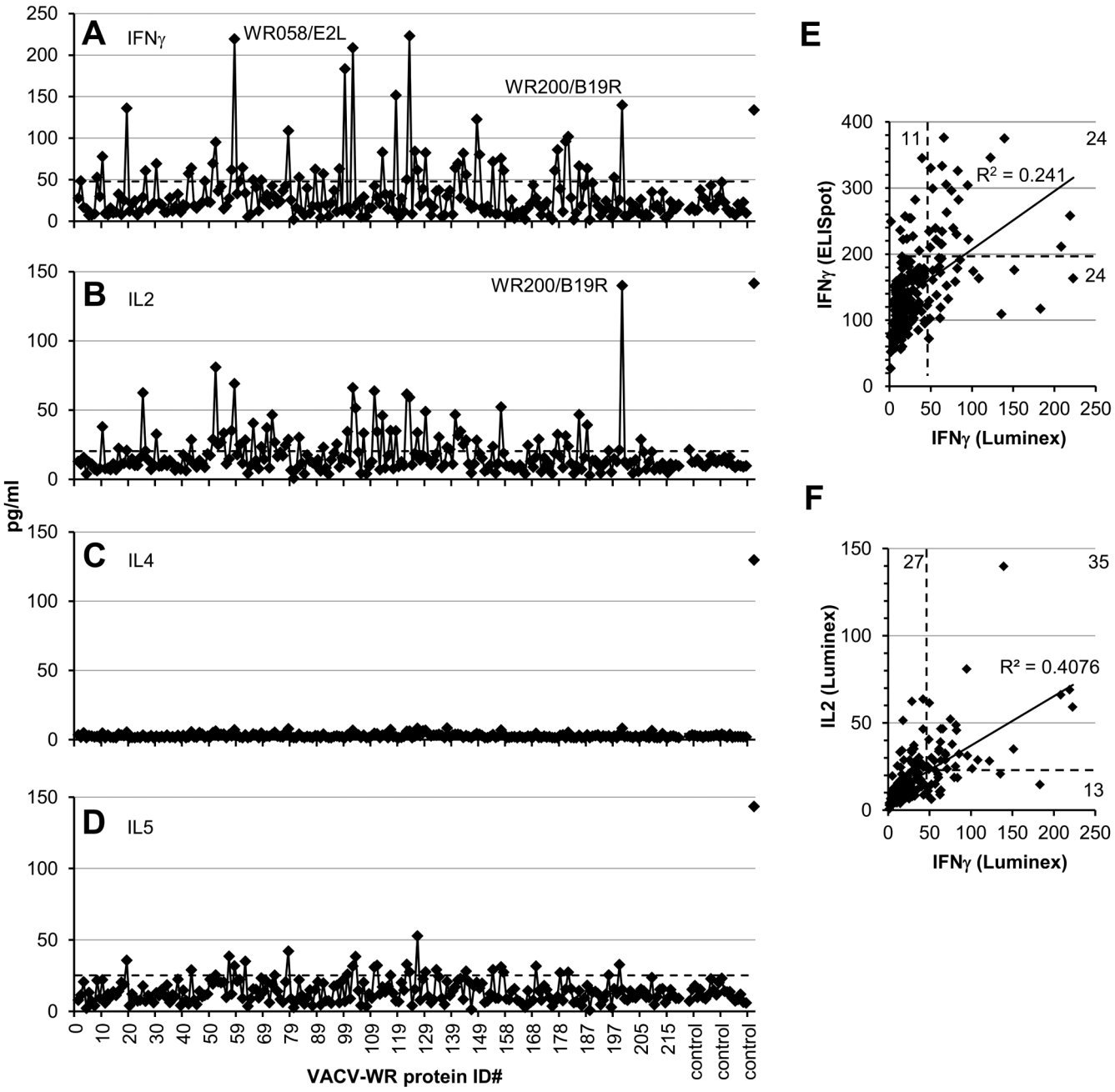

Figure 5. Proteome-wide screen of splenocytes from VACV-WR infected mice by Luminex® assay for secreted signature cytokines of Th1 and Th2 cells

Supernatants from the ELISpot depicted in Fig. 4B were assayed for Th1 cytokines IFNγ and IL2, and Th2 cytokines IL4 and IL5 by Luminex® MAGPIX® system. **A**, IFNγ; **B**, IL2; **C**, IL4; **D**, IL5. The spot to the right of each plot is a positive control sample for each cytokine. **E,** scatter plot of supernatant vs. spot assays for IFNγ. **F**, scatter plot of supernatant assays for IFNγ vs. IL2. Hashed lines, cutoff defined as average + 2.5 SD of control wells containing *P. falciparum* and *F. tularensis* antigens. Values in the scatter plots represent number of antigens in each quadrant.

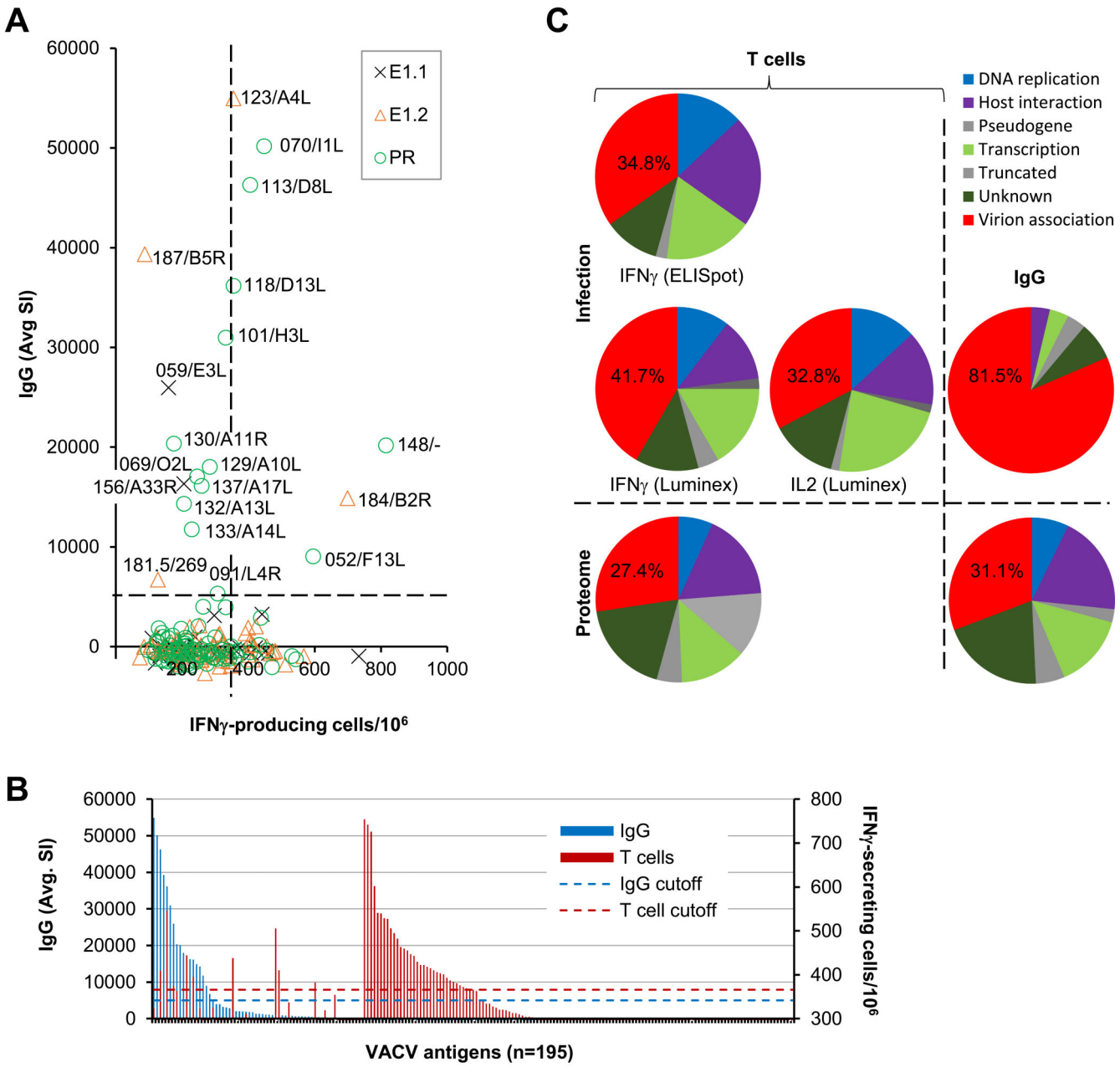

Figure 6. Comparisons between T cell and antibody target antigen profiles

A. Scatter plots of IgG signals by microarray vs. corresponding T cell responses from representative IFNγ ELISPOT. Cut-offs (hashed lines); for T cells defined as mean+2.5SD of control antigens (n=35; SDS-IBs proteome n = 225); antibody targets antigens defined as described in Table 2 (n=26; proteome on array n=194). Different temporal expressions indicated by symbols, as defined by Yang et al (32) using cluster analysis of viral mRNAs at 0.5, 1, 2 and 4h infection time points: E1.1=early subcluster 1; E1.2=early subcluster 2; PR=post-replicative. **B**. Bar charts of antibody signals (average of 6 mice) and T cells (averages of spot-forming cells/10^6 on d8 and d13, as shown in Fig 4). The first 65 antigens are ranked by antibody signal and thereafter by T cell response. **C**. Pie charts showing

proportions of reactive antibody and CD4 T cell targets, compared to the whole VACV-WR proteome. Each protein was classified into a functional category according to Yang et al (2010) (32). Note: most of the pseudogenes were omitted from the arrays, so the proteome pie charts for IgG and for the T cell screens differ slightly.

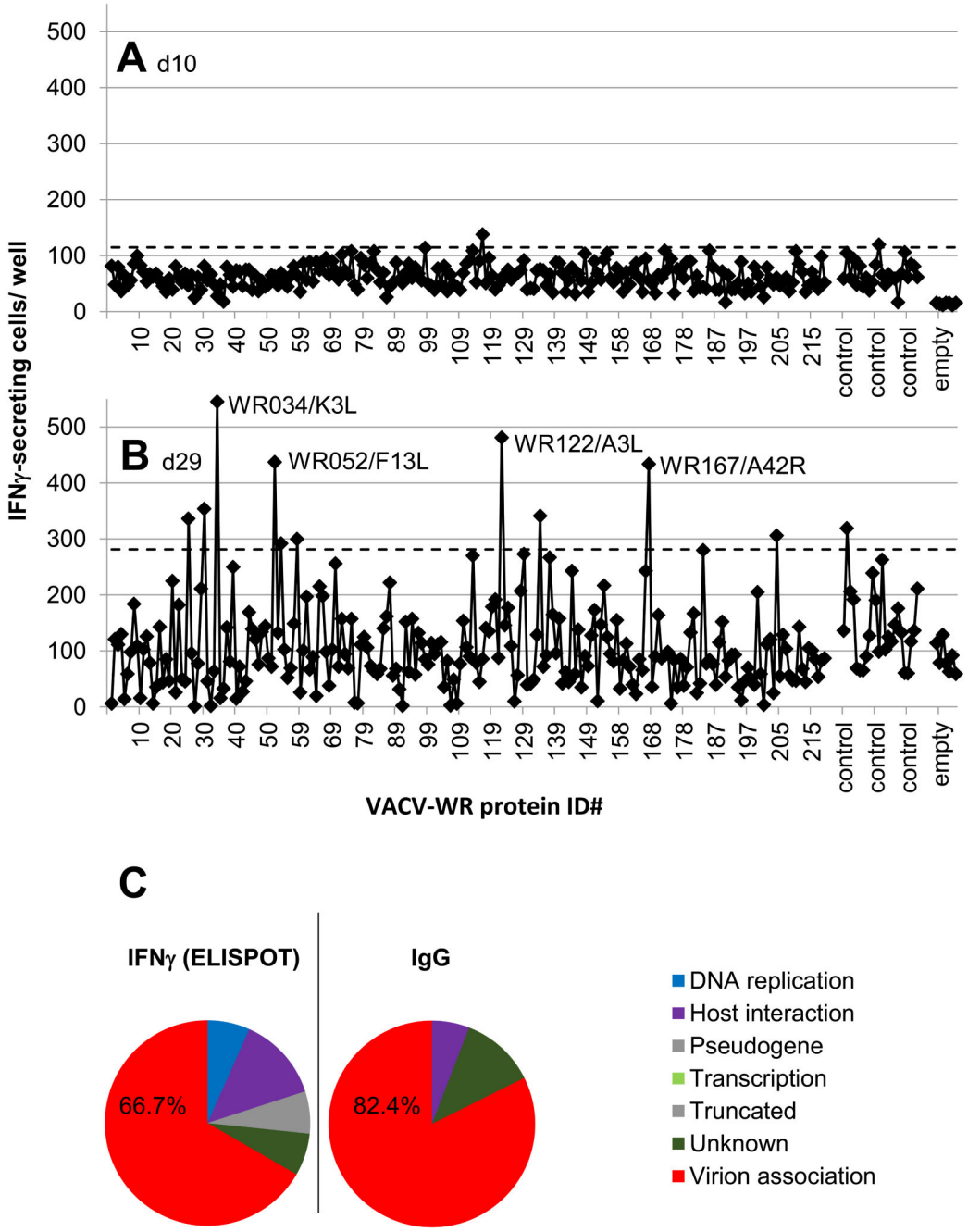

Figure 7. Comparisons between T cell and antibody target antigen profiles in response to heat-inactivated VACV-WR

C57Bl/6 mice were administered i.p. heat-inactivated VACV-WR (approx. 1×10^7 pfu equivalents/mouse) in alum on d0 and challenged i.n. on d22. Spleen cells from three mice were pooled on d10 and d29 and subjected to IFNγ ELISPOTs against the full SDS-IB VACV-WR proteome as described in Fig. 4. **A**, ELISPOT data from d10, after heat inactivated VACV-WR i.p. prime only. **B**, ELISPOT data from d29, after heat inactivated VACV-WR i.p. prime and 'live' VACV-WR i.n. boost. Four immunodominant antigens are

highlighted for orientation. **C**. Pie charts showing proportions of reactive antibody and T cell targets on d29. Whole VACV-WR proteomes for comparison shown in Fig. 5.

Table 1
Top T cell antigens defined by two IFNγ-release assays

Gene [a]	Protein Product [b]	Functional Category [c]	Exp [d]	Prom [e]	ELISpot rank [f]	Luminex rank [g]
WR200\B19R	IFNα/β receptor-like secreted glycoprotein	Host interact	E1.1	E	2	6
WR148\−	cowpox A-type inclusion protein	Virion assoc	PR	L	3	8
WR058\E2L	hypothetical protein	Virion assoc	E1.2	L	15	2
WR052\F13L	palmytilated EEV membrane glycoprotein	Virion assoc	PR	L	9	12
WR113\D8L	IMV membrane protein	Virion assoc	PR	L	7	15
WR184\B2R	hypothetical protein	Truncated	E1.2	E/L	1	25
WR125\A6L	hypothetical protein	Virion assoc	PR	L	12	14*
WR156\A33R	EEV membrane phosphoglycoprotein	Virion assoc	E1.1	E/L	11	20
WR140\A21L	IMV membrane protein	Virion assoc	PR	L	5	27
WR030\M1L	ankyin-like protein	Unknown	E1.2	E	8	24
WR102\H4L	RAP94	Transcription	PR	L	33	3
WR141\A20R	viral DNA polymerase processivity factor	DNA replic	E1.2	E	14	22
WR010\C10L	hypothetical protein	Host interact	E1.2	E	20	19
WR180\A55R	kelch-like protein	Host interact	E1.2	L	29	11
WR143\A23R	45kDa large subunit of intermediate gene transcription factor VITF-3	Transcription	E1.2	E	25	17
WR122\A3L	p4b precursor of core protein 4b	Virion assoc	PR	L	6	43
WR082\G5R	Hypothetical protein	DNA replic	E1.2	E	10	40
WR061\E5R	Hypothetical protein	Unknown	E1.1	E	24	26*
WR043\F4L	ribonucleotide reductase small subunit	DNA replic	E1.2	E	31	28
WR144\A24R	DNA-dependent RNA polymerase subunit rpo132	Transcription	E1.2	E/L	21	39
WR097\J5L	late 16kDa putative membrane protein	Virion assoc	PR	E/L	32	30*
WR091\L4R	DNA-binding virion core protein	Transcription	PR	L	28	38
WR060\E4L	RNA polymerase subunit	Transcription	E1.1	E/L	23	46
WR065\E9L	DNA polymerase	DNA replic	E1.2	E	34	44
WR123\A4L	39kDa core protein	Virion assoc	E1.2	L	<	1
WR099\H1L	tyr/ser protein phosphatase	Transcription	PR	L	<	4*
WR118\D13L	rifampicin target	Virion assoc	PR	L	<	5
WR019\C9L	ankyrin-like protein	Unknown	E1.2	E	<	7
WR078\G1L	putative metalloprotease	Virion assoc	PR	L	<	9
WR181\A56R	hemagglutinin	Virion assoc	E1.2	E/L	<	10
WR177\A51R	hypothetical protein	Unknown	E1.1	E	<	13
WR129\A10L	precursor p4a of core protein 4a	Virion assoc	PR	L	<	16
WR149\A26L	cowpox A-type inclusion protein	Virion assoc	PR	L	<	18*

Gene [a]	Protein Product [b]	Functional Category [c]	Exp [d]	Prom [e]	ELISpot rank [f]	Luminex rank [g]
WR153.5\ A30.5L	hypothetical protein	Unknown	PR	L	<	21
WR051\F12L	EEV maturation protein	Virion assoc	E1.2	E	<	23
WR187\B5R	EEV membrane glycoprotein	Virion assoc	E1.2	E/L	<	29
WR088\L1R	IMV membrane protein	Virion assoc	PR	L	<	31*
WR057\E1L	poly(A) polymerase large subunit	Transcription	E1.2	E/L	<	32
WR126\A7L	82kDa large subunit of early gene transcription factor VETF	Transcription	PR	L	<	33
WR157\A34R	IEV and EEV membrane glycoprotein	Virion assoc	PR	L	<	34*
WR176\A50R	ATP-dependent DNA ligase	DNA replic	E1.2	E	<	35*
WR026\C2L	kelch-like protein	Host interact	E1.2	E/L	<	36
WR042\F3L	Kelch-like protein	Host interact	E1.2	L	<	37*
WR008\C19L	ankyrin-like protein	Truncated	PR	E/L	<	42*
WR197\B15R	IL-beta-binding protein	Host interact	PR	L	<	41*
WR068\O1L	Hypothetical protein	Unknown	E1.1	E	<	45
WR002\−	TNF-alpha-receptor-like protein	Pseudogene	E1.2	E	<	47*
WR048\F9L	S-S bond formation pathway protein	Virion assoc	PR	E/L	<	48*
WR085\G7L	putative viron core protein	Virion assoc	PR	L	4	<
WR070\I1L	putative DNA-binding virion core protein	Virion assoc	PR	L	13	<
WR170\A44L	hydroxysteroid dehydrogenase	Host interact	E1.2	E	16	<
WR205\C12L	serine protease inhibitor-like SPI-1	Host interact	E1.2	E	18	<
WR022\C6L	hypothetical protein	Unknown	E1.1	E	17	<
WR080\G2R	transcriptional elongation factor	Transcription	E1.2	E	19	<
WR098\J6R	DNA-dependent RNA polymerase subunit rpo147	Transcription	E1.2	E/L	22	<
WR025\C3L	secreted complement-binding protein	Host interact	PR	L	26	<
WR167\A42R	profilin-like protein	Virion assoc	PR	L	27	<
WR195\B13R	SPI-2/CrmA inhibits Fas-mediated apoptosis, IL-1 convertase, lipoxygenase pathway	Host interac	E1.1	E	30	<
WR076\I7L	viral core cysteine proteinase	Virion assoc	PR	L	35	<

[a] Complete list of reactive antigens defined by ELISpot and bead-capture (Luminex) assays for IFNγ. Antigens are defined as positive if the number of spots (in ELISpot) or pg/ml (in Luminex assays) > means+2.5 SD of the corresponding values in 24 control antigen wells. Antigens defined as positive in both assays (n=24) are shown in the top section of the table and are ranked by the aggregate rank of each assay. Antigens defined as hits by luminex only (n=24) and by ELISpot only (n=11) are shown in the middle and bottom sections, respectively. Gene nomenclature is a concatenation of VACV-WR (Western Reserve) and the VACV-COP (Copenhagen) orthologs. Bold = one of 13 CD4 T cell antigens described by Moutaftsi et al (70).

[b] Descriptions of protein products from www.poxvirus.org and updated from the literature.

[c] Functional categories defined by Yang et al (32) based on definitions in the literature. DNA replic, DNA replication; Host interac, host interaction; Virion assoc, vision associated;

[d] Expression. Temporal expression defined by Yang et al (32) using cluster analysis of viral mRNAs at 0.5, 1, 2 and 4h infection time points. E1.1=early subcluster 1; E1.2=early subcluster 2; PR=post-replicative.

[e] Promoter. Consensus promoter type derived from www.poxvirus.org, deep sequencing (32), and transcriptomic analyses (84, 85).

[f] Rank number (where 1 = highest) determined by ranking antigens by number of spots/well in descending order from assay shown in Fig 4B; <, below cutoff defined as mean + 2.5SD of control antigens.

[g] Rank number (where 1 = highest) determined by ranking antigens by number of pg/ml in descending order from assay shown in Fig 5A; <, below cutoff defined as mean + 2.5SD of control antigens. Asterisks indicate antigens positive for IFNγ but negative for IL2 in Luminex assays of the same culture supernatant (n=13; see Fig 5F).

Table 2
Top T cell antigens defined by IL2 secretion (Luminex®) assay

Gene[a]	Protein Product[b]	Functional Category[c]	Exp[d]	Prom[e]
WR200\B19R	IFN-alpha/beta-receptor-like secreted glycoprotein	Host interaction	E1.1	E
WR052\F13L	palmytilated EEV membrane glycoprotein	Virion association	PR	L
WR058\E2L	hypothetical protein	Virion association		L
WR102\H4L	RAP94	Transcription	PR	L
WR122\A3L	p4b precursor of core protein 4b	Virion association	PR	L
WR123\A4L	39kDa core protein	Virion association		L
WR156\A33R	EEV membrane phosphoglycoprotein	Virion association	E1.1	E/L
WR129\A10L	precursor p4a of core protein 4a	Virion association	PR	L
WR184\B2R	hypothetical protein	Truncated	E1.2	E/L
WR140\A21L	IMV membrane protein	Virion association	PR	L
WR113\D8L	IMV membrane protein	Virion association	PR	L
WR065\E9L	DNA polymerase	DNA replication	E1.2	E
WR187\B5R	EEV membrane glycoprotein	Virion association	E1.2	E/L
WR010\C10L	hypothetical protein	Host interaction		E
WR057\E1L	poly(A) polymerase large subunit	Transcription	E1.2	E/L
WR118\D13L	rifampicin target	Virion association	PR	L
WR126\A7L	82kDa large subunit of early gene transcription factor VETF	Transcription	PR	L
WR030\M1L	ankyin-like protein	Unknown	E1.2	E
WR177\A51R	hypothetical protein	Unknown	E1.1	E
WR141\A20R	viral DNA polymerase processivity factor	DNA replication	E1.2	E
WR180\A55R	kelch-like protein	Host interaction	E1.2	L
WR082\G5R	Hypothetical protein	DNA replication	E1.2	E
WR051\F12L	EEV maturation protein	Virion association	E1.2	E
WR078\G1L	putative metalloprotease	Virion association	PR	L
WR043\F4L	ribonucleotide reductase small subunit	DNA replicaton	E1.2	E
WR144\A24R	DNA-dependent RNA polymerase subunit rpo132	Transcription	E1.2	E/L
WR148\−	cowpox A-type inclusion protein	Virion association	PR	L
WR143\A23R	45kDa large subunit of intermediate gene transcription factor VITF-3	Transcription	E1.2	E
WR060\E4L	RNA polymerase subunit	Transcription	E1.1	E/L
WR181\A56R	hemagglutinin	Virion association	E1.2	E/L
WR153.5\A30.5L	hypothetical protein	Unknown	PR	L
WR068\O1L	Hypothetical protein	Unknown	E1.1	E
WR091\L4R	DNA-binding virion core protein	Transcription	PR	L
WR019\C9L	ankyrin-like protein	Unknown	E1.2	E
WR026\C2L	kelch-like protein	Host interaction	E1.2	E/L
WR110\D5R	NTPase	DNA replication	E1.2	E/L

Gene[a]	Protein Product[b]	Functional Category[c]	Exp[d]	Prom[e]
WR025\C3L	secreted complement-binding protein	Host interaction	PR	L
WR103\H5R	late transcription factor VLTF-4	Transcription	E1.1	E/L
WR072\I3L	DNA-binding phosphoprotein	DNA replication	E1.1	E/L
WR070\I1L	putative DNA-binding virion core protein	Virion association	PR	L
WR116\D11L	ATPase, nucleoside triphosphate phosphohydrolase-I, NPH-I	Transcription	PR	L
WR142\A22R	palmitylprotein	DNA replication	PR	L
WR100\H2R	putative viral membrane protein	Virion association	PR	L
WR111\D6R	70kDa small subunit of early gene transcription factor VETF	Transcription	PR	L
WR106\D1R	large subunit of mRNA capping enzyme	Transcription	E1.2	E
WR054\F15L	hypothetical protein	Unknown	E1.1	E
WR134\A14.5L	hydrophobic IMV membrane protein	Virion association	PR	L
WR170\A44L	hydroxysteroid dehydrogenase	Host interaction	E1.2	E
WR205\C12L	serine protease inhibitor-like SPI-1	Host interaction	E1.2	E
WR062\E6R	Hypothetical protein	Virion association	PR*	L
WR073\I4L	ribonucleotide reductase large subunit	DNA replication	E1.2	E
WR053.5\F14.5L	hypothetical protein	Virion association	E1.2	E/L
WR096\J4R	DNA-dependent RNA polymerase subunit rpo22	Transcription	E1.2	E
WR053\F14L	hypothetical protein	Unknown	E1.1	E
WR077\I8R	RNA helicase NPH-II	Transcription	PR	E/L
WR166\A41L	secreted glycoprotein	Host interaction	E1.2	E
WR137\A17L	IMV membrane protein	Virion association	PR	L
WR016\−	ankyrin-like protein	Pseudogene	E1.2	E/L
WR138\A18R	DNA helicase	Transcription	E1.2	E/L
WR199\B18R	ankyrin-like protein	Unknown	E1.2	E/L
WR195\B13R	SPI-2/CrmA inhibits Fas-mediated apoptosis, IL-1 convertase	Host interaction	E1.1	E

[a] As per Table 1. Antigens that were defined as positive by both IL2 and IFNγ assays (n=35) are shown in the top section of the table, whereas those positive by IL2 but not IFNγ (n=26) shown in the lower section. In each section, the antigens are ranked in descending order by quantity of IL2 detected (pg/ml). Antigens negative for IL2 but positive for IFNγ (n=13) are indicated in Table 1.

[b] Descriptions of protein products from www.poxvirus.org and updated from the literature.

[c] Functional categories defined by Yang et al (32) based on definitions in the literature. DNA replic, DNA replication; Host interac, host interaction; Virion assoc, vision associated;

[d] Expression. Temporal expression defined by Yang et al (32) using cluster analysis of viral mRNAs at 0.5, 1, 2 and 4h infection time points. E1.1=early subcluster 1; E1.2=early subcluster 2; PR=post-replicative.

[e] Promoter. Consensus promoter type derived from www.poxvirus.org, deep sequencing (32), and transcriptomic analyses (84, 85).

Table 3
Dominant antigens recognized by immune serum IgG in response to VACV-WR infection

Gene[a]	Protein product[b]	Functional category[c]	Expression[d]	Promoter[e]	IMV[f]	IMV[g]
WR123/A4L	39kDa core protein	Virion association	E1.2	L	5	1
WR070/I1L	putative DNA-binding virion core protein	Virion association	PR	L	35	53
WR113/D8L	IMV membrane protein	Virion association	PR	L	10	12
WR187/B5R	EEV membrane glycoprotein	Virion association	E1.2	E/L	-	-
WR118/D13L	rifampicin target	Virion association	PR	L	70	71
WR101/H3L	IMV heparin binding surface protein	Virion association	PR	L	13	9
ssWR044/F5L	hypothetical protein	Unknown	E1.2	E	-	-
WR059/E3L	double-strand RNA-binding protein	Host interaction	E1.1	E	29	-
WR130/A11R	hypothetical protein	Virion association	PR	L	62	-
WR148/-	cowpox A-type inclusion protein	Virion association	PR	L	74	7
ssWR087/G9R	poxvirus myristoylprotein	Virion association	PR	L	55	65
WR129/A10L	precursor p4a of core protein 4a	Virion association	PR	L	7	2
WR069/O2L	glutaredoxin	Unknown	PR	L	34	35
WR156/A33R	EEV membrane phosphoglycoprotein	Virion association	E1.1	E/L	-	-
WR137/A17L	IMV membrane protein	Virion association	PR	L	2	44
WR184/B2R	hypothetical protein	Truncated	E1.2	E/L	-	-
ssWR134/A14.5L	hydrophobic IMV membrane protein	Virion association	PR	L	-	-
ssWR074/I5L	Hypothetical protein	Virion association	PR	L	-	63
WR132/A13L	IMV membrane protein	Virion association	PR	L	11	14
WR133/A14L	phosphorylated IMV membrane protein	Virion association	PR	L	6	8
WR052/F13L	palmytilated EEV membrane glycoprotein	Virion association	PR	L	67	
ssWR088/L1R	IMV membrane protein	Virion association	PR	L	22	56
ssWR159/A36R	IEV transmembrane phosphoprotein	Virion association	E1.1	E/L	-	-
ssWR113/D8L	IMV membrane protein	Virion association	PR	L	10	12
ssWR132/A13L	IMV membrane protein	Virion association	PR	L	11	14
WR181.5/269	hypothetical protein	Truncated	E1.2	E/L	-	-
ssWR079/G3L	Hypothetical protein	Virion association	?	?	?	?
WR091/L4R	DNA-binding virion core protein	Transcription	?	?	?	?

[a] As per Table 1. Antigens are ranked by average signal intensity on arrays probed with sera from 8 mice infected with VACV-WR via i.p. route and boosted with VACV-WR on d14 by i.n. route; sera were collected on d21 for array probing. Only seropositive antigens (average protein array

signal intensity >5000) shown. Antigens with the prefix “ss” were expressed in the RTS- disulfide kit; antigen WR113/D8L and WR132/A13L is present twice in the table.

[b] Descriptions of protein products from www.poxvirus.org and updated from the literature.

[c] Functional categories defined by Yang et al (32) based on definitions in the literature. DNA replic, DNA replication; Host interac, host interaction; Virion assoc, vision associated;

[d] Expression. Temporal expression defined by Yang et al (32) using cluster analysis of viral mRNAs at 0.5, 1, 2 and 4h infection time points. E1.1=early subcluster 1; E1.2=early subcluster 2; PR=post-replicative.

[e] Promoter. Consensus promoter type derived from www.poxvirus.org, deep sequencing (32), and transcriptomic analyses (1, 64).

[f] IMV components defined by mass spectroscopy, with ranking by mass (86).

[g] IMV components defined by mass spectroscopy, with ranking by mass (87).

Table 4

Top T cell antigen hits in mice receiving inactivated VACV-WR prime followed by live VAC-WR boost

Gene[a]	Protein Product[b]	Functional category[c]	Expr.[d]	Promoter[e]	IMV[f]	IMV[g]
WR140/A21L*	IMV membrane protein	Virion association	PR	L	?	?
WR034/K3L	interferon resistance protein	Host interaction	E1.1	E	-	-
WR122/A3L*	p4b precursor of core protein 4b	Virion association	PR	L	3	4
WR052/F13L*	palmytilated EEV membrane glycoprotein	Virion association	PR	L	67	-
WR167/A42R*	profilin-like protein	Virion association	PR	L	39	19
WR156/A33R*	EEV membrane phosphoglycoprotein	Virion association	E1.1	E/L	-	-
WR123/A4L*	39kDa core protein	Virion association	E1.2	L	5	1
WR030/M1L*	ankyin-like protein	Unknown	E1.2	E	63	-
WR134/A14.5L	hydrophobic IMV membrane protein	Virion association	PR	L	-	-
WR025/C3L*	secreted complement-binding protein	Host interaction	PR	L	-	-
WR204/-	hypothetical protein	Pseudogene	E1.2	E/L	-	-
WR129/A10L*	precursor p4a of core protein 4a	Virion association	PR	L	7	2
WR058/E2L*	hypothetical protein	Virion association	E1.2	L	-	-
WR053.5/F14.5L	hypothetical protein	Virion association	E1.2	E/L	-	-
WR183/B1R	ser/thr kinase	DNA replication	E1.2	E	79	-
WR113/D8L*	IMV membrane protein	Virion association	PR	L	10	12
WR137A17L	IMV membrane protein	Virion association	PR	L	2	44

[a] as per Table 1. Antigens are ranked by the number of spot forming cells in the IFN-γ ELISPOT assay depicted in Fig. 6A. Antigens were defined as hits if the number of spots > means+2SD of the number of spots in control antigen wells. Antigens recognized in VACV-WR infection in IFNγ assays (Table 1) are indicated by an asterisk.

[b] Descriptions of protein products from www.poxvirus.org and updated from the literature.

[c] Functional categories defined by Yang et al (83) based on definitions in the literature. DNA replic, DNA replication; Host interac, host interaction; Virion assoc, vision associated;

[d] Expression. Temporal expression defined by Yang et al (32) using cluster analysis of viral mRNAs at 0.5, 1, 2 and 4h infection time points. E1.1=early subcluster 1; E1.2=early subcluster 2; PR=post-replicative.

[e] Promoter. Consensus promoter type derived from www.poxvirus.org, deep sequencing (32), and transcriptomic analyses (84, 85).

[f] IMV components defined by mass spectroscopy, with ranking by mass (86).

[g] IMV components defined by mass spectroscopy, with ranking by mass (87).

Table 5

Dominant antigens recognized by immune serum IgG after inactivated VACV-WR prime followed by live VAC-WR boost

Gene [a]	Protein Product [b]	Functional category [c]	Expression [d]	Promoter [e]	IMV [f]	IMV [g]
WR113/D8L	IMV membrane protein	Virion association	PR	L	10	12
WR070/I1L	putative DNA-binding virion core protein	Virion association	PR	L	35	53
WR148/-	cowpox A-type inclusion protein	Virion association	PR	L	74	7
WR187/B5R	EEV membrane glycoprotein	Virion association	E1.2	E/L	-	-
WR137/A17L	IMV membrane protein	Virion association	PR	L	2	44
WR181/A56R	hemagglutinin	Virion association	E1.2	E/L	-	-
WR123/A4L	39kDa core protein	Virion association	E1.2	L	5	1
WR118/D13L	rifampicin target	Virion association	PR	L	70	71
WR132/A13L	IMV membrane protein	Virion association	PR	L	11	14
WR133/A14L	phosphorylated IMV membrane protein	Virion association	PR	L	6	8
ssWR044/F5L	hypothetical protein	Unknown	E1.2	E	-	-
ssWR162/A38L	CD47-like putative membrane protein	Virion association	PR	L	-	-
WR156/A33R	EEV membrane phosphoglycoprotein	Virion association	E1.1	E/L	-	-
WR178/A52R	Toll/IL-receptor-like protein	Host interaction	E1.2	E/L	-	-
WR069/O2L	glutaredoxin	Unknown	PR	L	34	35
WR058/E2L	hypothetical protein	Virion association	E1.2	L	-	-
WR101/H3L	IMV heparin binding surface protein	Virion association	PR, E	L	13	9

[a] As per Table 1. Antigens are ranked by average signal intensity on VACV protein arrays. Antigens with the prefix “ss” were expressed in the RTS-disulfide kit.

[b] Descriptions of protein products from www.poxvirus.org and updated from the literature.

[c] Functional categories defined by Yang et al (32) based on definitions in the literature. DNA replic, DNA replication; Host interac, host interaction; Virion assoc, vision associated;

[d] Expression. Temporal expression defined by Yang et al (32) using cluster analysis of viral mRNAs at 0.5, 1, 2 and 4h infection time points. E1.1=early subcluster 1; E1.2=early subcluster 2; PR=post-replicative.

[e] Promoter. Consensus promoter type derived from www.poxvirus.org, deep sequencing (32), and transcriptomic analyses (1, 64).

[f] IMV components defined by mass spectroscopy, with ranking by mass (86).

[g] IMV components defined by mass spectroscopy, with ranking by mass (87).